Reviewed Preprint
v1 • May 27, 2026
Not revised

For correspondence:
alex.schmidt@unibas.ch
anne.spang@unibas.ch

Competing interests: No competing interests declared

Funding: See page 24

Reviewing editor: Ishier Raote, Institut Jacques Monod, France

SPEx: Compartment-Resolved Proteomics via Expansion Microscopy–Guided Microdissection

Curdin A Franziscus, Alexia Ferrand, Oliver Biehlmaier, Alexander Schmidt, Anne Spang
Biozentrum, University of Basel, Basel, Switzerland

eLife Assessment

This is an **important** study describing 'SPEx', a broadly accessible method that combines cell expansion, laser microdissection, and mass spectrometry to enable subcellular proteomic profiling. The authors provide **convincing** evidence that this flexible integration of established techniques provides a robust and practical approach for compartment-resolved spatial proteomics. The authors support their main claims with appropriate validation across multiple subcellular compartments and show that the method can recover known markers while also identifying previously uncharacterized components. Overall, the work is likely to be of broad interest to cell and molecular biologists, particularly those seeking scalable and cost-effective strategies for mapping organelle composition.

https://doi.org/10.7554/eLife.111393.1.sa3

Abstract

Cells contain different organelles and compartments that are essential for cellular function and life. These organelles and compartments need to communicate to assess cellular state in a changing environment, adapt to the new situation, and also to ensure functionality and homeostasis. Moreover, organization and communication differ between cell types. However, our knowledge about these changes is still rather scarce. Subcellular spatial proteomics aims to fill this knowledge gap. While proximity labeling techniques represent a great advance, they do not provide precise spatial resolution. To overcome this limitation, we developed SPEx (**S**ubcellular spatial **P**roteomics coupled to **Ex**pansion), in which we first expand cells about 10– fold, laser micro-dissect regions of interests and then perform mass spectrometry-based proteomics on these samples. We demonstrate the effectiveness of SPEx by determining the proteome of the Golgi, the nucleus and nucleoli. Satisfyingly, we also identify novel components of these organelles. Combining inexpensive already existing technologies makes SPEx readily usable by the wider scientific community.

Introduction

Intracellular communication is essential for any life form. The communication, however, changes depending on a multitude of inputs such as extracellular cues, cell-cycle stage, nutrient availability, stress and age. This adaptability is key to the survival of any organism. While our understanding is increasing about intracellular communication in a few model organisms, such as tissue culture cells, Drosophila, *C. elegans* and yeast in unperturbed conditions, we still lack understanding how communication changes under different conditions and in different cell types. Efforts to fill this knowledge gap are hampered by fact that the basic machinery is mostly the same, but often with variations in the interaction complexes, or under specific regulation in time and space, making the full picture hard to grasp.

Spatial subcellular proteomics intends to overcome this knowledge gap and aims to determine the localizations, concentrations and interactions of proteins within cells and tissues, while preserving their spatial information (Lundberg and Borner, 2019). A number of techniques have been developed to perform spatial proteomics at a subcellular resolution including differential centrifugation, organellar immunoprecipitation and proximity labeling methods (Fasimoye et al., 2023; Geladaki et al., 2019; Hundley et al., 2024; Lundberg and Borner, 2019; Roux et al., 2012). These techniques greatly improved our understanding of cellular organization and allowed the creation of comprehensive databases where large parts of, for example, the human proteome is mapped to specific subcellular compartments. However, all of these approaches identify proteins based on proximity or co-purification with known markers and not on actual spatial positional information. This shortcoming cannot be circumvented since these techniques rely on a lysis step prior to proteomic analysis and hence all spatial information is inevitably lost.

More recently, Microscoop® aimed to overcome these drawbacks by introducing a technique that allows laser-guided biotinylation of specific subcellular regions *in situ*, whose protein content can be determined by subsequent biotin pulldown and liquid chromatography – mass spectrometry (LC-MS) based proteomic analysis (Chang et al., n.d.; Chen et al., 2023). While allowing for high spatial resolution, the laser-guided biotinylation of the region of interest (ROIs) is very time consuming and expensive. The subsequent affinity purification step requires the labeling of a rather large number of ROIs and cells, contributing to the substantial costs and low-throughput. Because of the large number of required ROIs, this technique critically depends on automatization through machine learning algorithms and highly specialized equipment that are not readily available in most universities and research institutes. While an interesting technology, these drawbacks might limit the accessibility of Microscoop® for the wider scientific community.

Conversely, laser microdissection (LMD) allows direct LC-MS analysis of ROIs of tissues, cells or subcellular regions, and does not require a time– and sample-consuming affinity purification step. This method has been successfully applied to determine the proteome of single cells within tissues (Herrera et al., 2020; Large et al., 2020; Rosenberger et al., 2025, 2023) and is already an established and available workflow in many proteomics laboratories. Despite its recent success, this method is limited by its laser beam diameter (0.5 – 1 µm) which only allows collection of samples ranging from to 5-10 µm in diameter (Domazet et al., 2008; Walavalkar et al., 2025). These limitations prevented its application for sub-cellular spatial proteomics apart from isolation of whole nuclei from expanded cells (Dong et al., 2024).

Here, we introduce SPEx (**S**ubcellular spatial **P**roteomics coupled to **Ex**pansion), a novel technique that extends the application of LMD and LC-MS analysis to sub-cellular ROIs by combining expansion of samples using a hydrogel with LMD. SPEx utilizes the well-established TREx protocol developed for expansion microscopy (ExM), allowing up to 10-fold expansion of cultured cells (Damstra et al., 2022). This expansion greatly increases the resolution of LMD and allows dissection of individual organelles at a single micrometer resolution. Furthermore, we demonstrate that SPEx allows the determination of the proteome of a diverse group of organelles differing in size and shape and can be used as a tool to identify novel proteins locating to distinct regions within the cell. Strikingly, with the introduction of ultra-sensitive LC-MS platforms designed for single cell analysis (Brunner et al., 2022; Guzman et al., 2024), reasonable proteome coverage can be obtained with as little as about two dozen organelles. Moreover, SPEx is highly versatile and circumvents the need of specific protocols to isolate different organelles or regions of the cell by exclusively relying on visual selection of ROIs, based on fluorescent antibodies and/or dyes. In summary, we present SPEx, a novel kit-free, inexpensive method allowing *in situ* spatial proteomics at a micrometer resolution, which requires only a low amount of material.

Results

Development of the SPEx method

To overcome the need for an accessible, inexpensive subcellular spatial proteomics method, we developed SPEx (Figure 1A). This method combines expansion microscopy, laser microdissection and LC/MS analysis. In a first step, cells are fixed and the cellular structure(s) of interest is/are labelled with antibodies as in standard immunofluorescence. In the present study, we labelled the Golgi apparatus with an anti-GM130 antibody, combined with a fluorescent N-hydroxysuccinimide (NHS) –ester to label all proteins non-specifically (Sheard et al., 2023). To efficiently dissect subcellular structures, we aimed for a robust expansion of about 10-fold, while preserving downstream compatibility to LC/MS proteomic analysis. A protein disruption step is necessary to suppress the non-covalent interactions in the cells. This step is typically a protease treatment (e.g. proteinase K), which is degrading proteins prior to expansion, allowing for high expansion factors (Chen et al., 2015; Tillberg et al., 2016; Wen et al., 2023) but making it incompatible with downstream LC-MS. SDS denaturation can be used as an alternative protein disruption, as described in the U-ExM or TREx protocols (Damstra et al., 2022; Gambarotto et al., 2019). To confirm that this alternative was suitable for LC/MS analysis, we tested whether such expanded samples after protein denaturation were still containing intact peptides that could be efficiently extracted from the gel. When we tested this compatibility, we also found that the sample size could be relatively small, while still maintaining good proteome coverage (Figure S1A and Supplementary table 1 and 2). However, while most of the ExM publications use protease treatment for disruption to reach the 10-fold expansion (Chen et al., 2015; Tillberg et al., 2016; Wen et al., 2023), SDS denaturation only gave us an expansion factor ranging from 4-7 fold, while the gels themselves expanded 10-fold. Due to this variability, we decided to adjust the TREx protocol (Damstra et al., 2022) to ensure a robust and high expansion factor. After reducing the anchoring between the proteins and matrix to a minimum, and performing an overnight denaturation at 95 °C, we consistently obtained ~9x expansion without protease treatment. At this expansion level, we still could detect the Golgi and also proteins labelled by the NHS ester (Figure 1B and C). Of note, the strongest staining with the NHS ester was observed in the nucleus, and in particular in nucleoli. Because the nuclei were strongly labeled by the NHS ester, we used the difference in nuclear diameter before and after expansion as a surrogate to determine the expansion factor (Liffner et al., 2024) (Figure 1D and E).

For the laser microdissection step, the aqueous properties of the gels were making the laser cutting, due to laser diffraction and strong surface tension, impossible. To overcome these issues, we dried the samples completely. This procedure conserved the fluorescence signal from both, NHS dyes as well as secondary antibodies on the PPS membrane slide, which is used for LMD (Figure 2A and B). To our surprise, drying of the gel did not lead to severe shrinkage in length and width (x-y direction), but only in height (z-direction) (Figure 2C and D). Thus, we routinely retained an expansion of about 7x in x-y direction. The dried gels allowed efficient cutting at subcellular resolution using a Leica LMD7 system (Figure 2E, Supplementary video 1). We concentrated our efforts on three different organelles: the nucleus, the membraneless nucleolus, which were both nicely stained with the NHS ester, and the Golgi apparatus, visualized with anti-GM130. A summary of the number of cells and organelles, and which magnification was used to cut cells and organelles, are outlined in Supplementary table 3. We did not only isolate these organelles from individual cells, but also excised the exact same cells from which the nucleus/Golgi apparatus were removed (CellsMinusNucleus/CellsMinusGolgi) (Figure 2E). Similarly, after sampling the nuceoli, we also cut the nuclei from which the nucleoli were taken (NucleiMinusNucleoli) (Figure 2E). This was only possible, because laser dissection allowed for repeated sampling from the same cell, without compromising sample quality. The collected samples were then prepared for proteomics, using an optimized protocol for low-input samples based on previous spatial proteomics workflows and latest generation of highly sensitive time-of-flight (ToF) LC-MS instrumentation using DIA-PASEF data acquisition (Makhmut et al., 2026; Rosenberger et al., 2025). We consistently detected between 1,200 and 2,800 proteins per sample

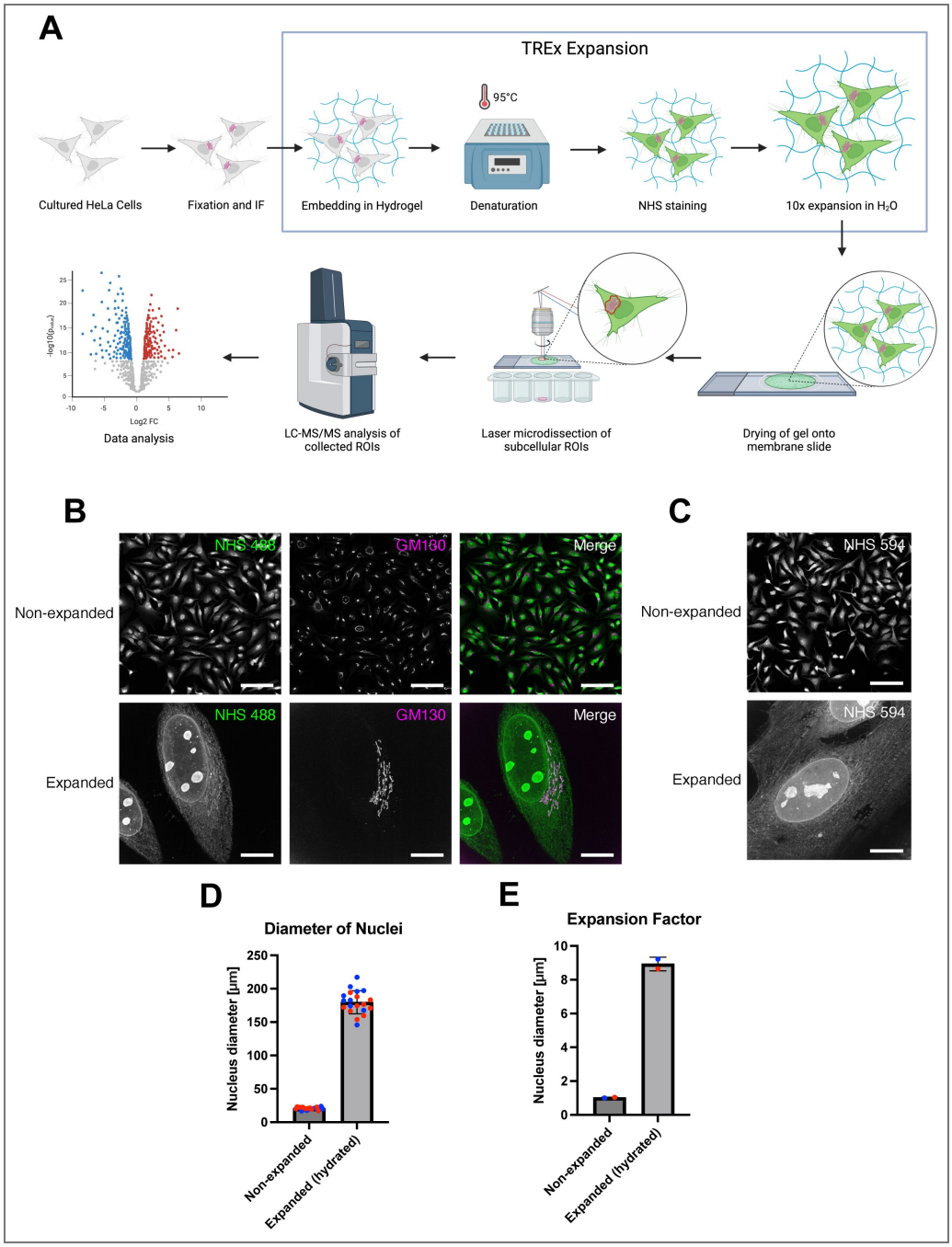

Figure 1. Development of the SPEx protocol

(A) SPEx workflow. Cultured HeLa cells are fixed, and immunofluorescence is used to label the subcellular compartment of interest with fluorescent antibodies. Next, the cells are embedded in a hydrogel. To allow for later expansion, proteins are denatured overnight at 95 °C. NHS staining is performed to non-specifically label proteins before expansion of the gel in H_2O. Expanded gels are dried onto PPS membrane slides, and laser microdissection of the areas of interest is performed. LC–MS of the collected areas and subsequent data analysis are used to identify proteins enriched in specific subcellular compartments. Created with *BioRender.com*. **(B)** Cells stained for total protein content with NHS 488 and immunostained with a GM130 antibody, with and without expansion using a modified TREx protocol. Scale bar: 100 µm. **(C)** Cells stained for total protein content with NHS 594, with and without expansion using a modified TREx protocol. Scale bar: 100 µm. **(D)** Measured nuclear diameters for expanded and non-expanded cells. Data are plotted as mean ± SD (non-expanded: 20.53 ± 1.94 µm; expanded (hydrated): 179.70 ± 17.26 µm) (n = 10 cells; N = 2 independent experiments indicated by different colors). **(E)** Average expansion factor calculated based on the measurements in (D). Data are plotted as mean ± SD (expanded (hydrated): 8.934 ± 0.40) (N = 2 independent experiments indicated by different colors).

(Figure 2F and Supplementary tables 4 and 5). As expected, the number of protein identifications correlated with organelle size, where whole cells had the highest and nucleoli the lowest number of proteins. Moreover, principal component analysis (PCA) revealed very good clustering of biological replicates and, with the exception of whole cell controls, distinct segregation of the different sample types (Figure 2G). Of note, the whole cell samples from the nuclei and Golgi experiments cluster nicely together, confirming robust proteome quantification of our SPEx workflow. Taken together, SPEx allows the expansion of cells, laser dissection of membrane-bounded and membraneless organelles and the detection of protein constituents in these organelles.

SPEx is suitable for the identification of nuclear proteins

To test the specificity and sensitivity of the SPEx method, we first applied it to the analysis of nuclear proteins from human HeLa cells. The NHS ester allows the visualization of the entire cell and nucleus, and, hence, we cut out 25 nuclei from expanded cells and subjected them to LC-MS analysis. In addition, we analyzed the proteome of either cut-out whole cells or the cut-outs of the same 25 cells from which the nuclei had been dissected (CellsMinusNuclei). These samples were subjected to LC-MS analysis. Next, we compared either whole cells or CellsMinusNuclei to the nuclei sample. As expected, we observed much stronger abundance differences and thus a higher number of significantly enriched nuclear proteins when comparing nuclei to CellsMinusNuclei rather than to WholeCells (Figure 3A and S1B). Moreover, the comparison of the proteome of the nuclei to the one of the remaining cells without nucleus minimizes cellular proteome variability. Using this comparison, we quantified around 2,200 proteins from only 25 nuclei (Figure 2F and Supplementary table 5), with 522 proteins being significantly enriched in the nuclear samples. To evaluate the specificity of our approach, we checked the proportion of nuclear annotated proteins according to GO (Supplementary table 6) in the enriched protein fraction. We found 499 of the 522 proteins to be annotated nuclear, corresponding to a very high specificity of more than 95% (Figure 3B). Gratifyingly, SPEx identified 23 proteins with strong nuclear enrichment that have not been annotated to be nuclear according to GO. Those proteins include SPOUT1 and C7orf50. Using immunofluorescence on non-expanded HeLa cells, we confirmed the nuclear localization of C7orf50 (Figure 3C) and SPOUT1 (Figure 4D) in HeLa cells, validating the high spatial specificity achieved with our approach. As an additional specificity test, we performed a functional enrichment analysis, which confirmed all top significantly enriched categories to be nuclear (Figure 3D and Supplementary table 7). Interestingly, this enrichment analysis also identified significantly depleted cellular compartments in our comparison, such as the plasma membrane and mitochondria (Figure 3E). Since cells without nuclei were used as a control for our analysis, SPEx can apparently not only be employed to localize proteins that are enriched in the nucleus, but also detect those that are specifically depleted and hence absent from the nuclear fraction. This effect is already evident in the volcano plot, as proteins that are exclusively present in the cytoplasm (DHX57), peripherally associated with non-nuclear organelles (Golgi: LRBA and FAM3C) or constituents of those organelles (mitochondria: TIMM8A) are among the most significantly depleted proteins (Figure 3A).

Many proteins annotated to be nuclear by GO have either also functions in the cytoplasm and/or partition between the nucleus and other cellular locations. The quantitative capabilities of SPEx allowed to define the primary location of a protein. Even if a protein is annotated to be nuclear by GO, but depleted in the nuclei sample, this protein is most likely in higher amount outside than inside the nucleus. For example, CLIP1 is annotated to be nuclear using GO. However, in our analysis, CLIP1 was strongly depleted from the nuclei (Figure 3A). In agreement with our findings, CLIP1 (CLIP-170) is a microtubule binding protein in the cytoplasm (Perez et al., 1999), also annotated as such in uniprot, proteinatlas and opencell (Cho et al., 2022; Nirschl et al., 2016; "The Human Protein Atlas," n.d.; The UniProt Consortium, 2025; Thul et al., 2017). Likewise, SNTB2 was annotated to be nuclear by GO. In contrast, it is annotated to be in the cytoplasm according to UniProt and has a confirmed localization in the cytoplasm/Golgi in the Human Protein Atlas. Moreover, SNTB2 has been localized to the cytoplasm in adipocytes (Krautbauer et al., 2019). Thus, we confidently detect proteins that are strongly depleted from

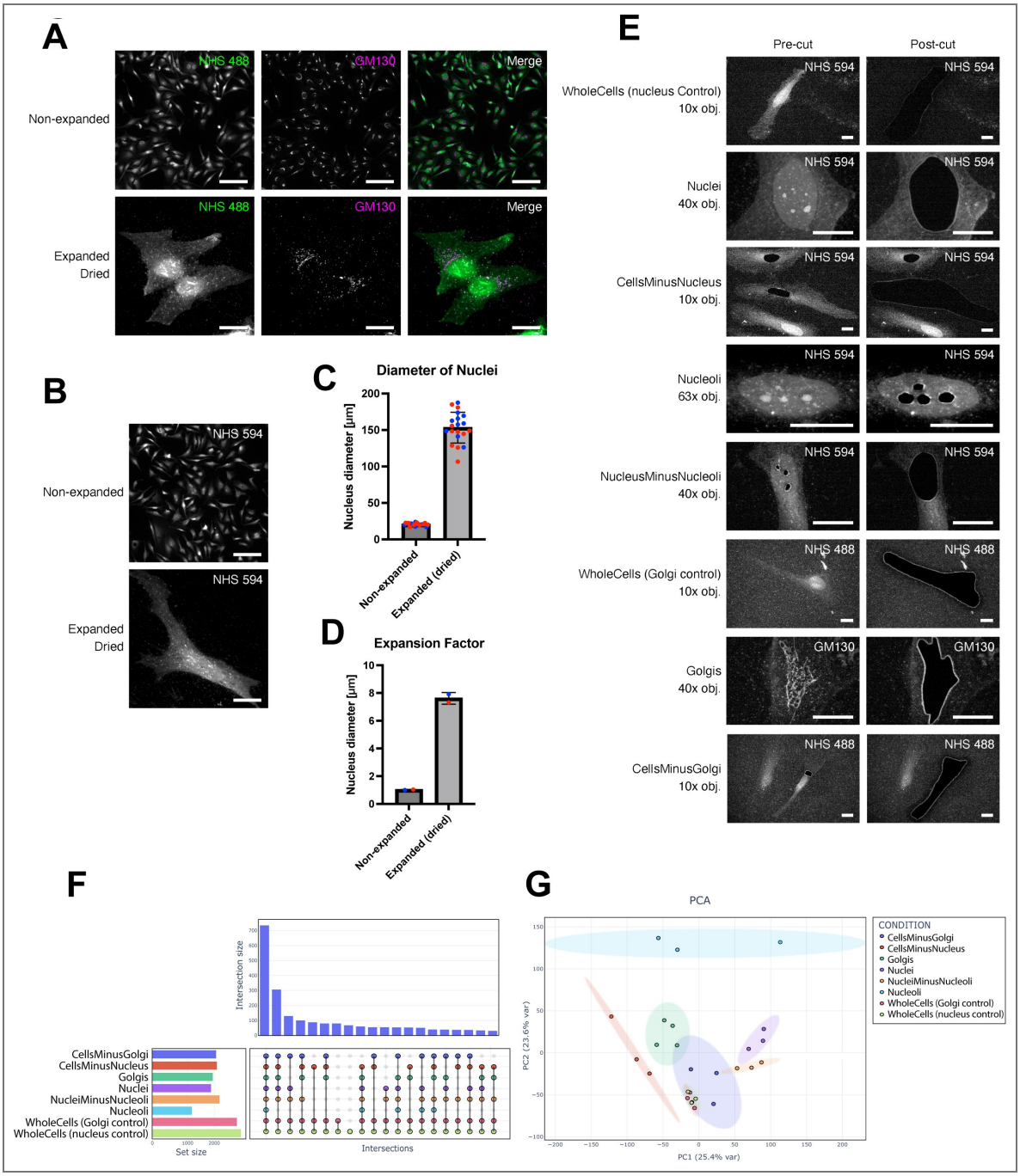

Figure 2. Optimization of the SPEx protocol for laser microdissection

(A) Cells stained for total protein with NHS 488 and immunostained for GM130, with and without expansion using a modified TREx protocol. Expanded samples were dried onto PPS membrane slides prior to imaging. Scale bar, 100 µm. **(B)** Cells stained for total protein with NHS 594, with and without expansion using a modified TREx protocol. Expanded samples were dried onto PPS membrane slides prior to imaging. Scale bar, 100 µm. **(C)** Nuclear diameters in expanded (dried) and non-expanded cells. Data are mean ± s.d. (non-expanded: 20.53 ± 1.94 µm; expanded (dried): 153.30 ± 21.16 µm; n = 10 cells, N = 2 independent experiments indicated by different colors). **(D)** Expansion factor calculated from measurements in (C). Data are mean ± s.d. (7.61 ± 0.42; N = 2 independent experiments indicated by different colors). **(E)** Pre– and post-cut images of all isolated sample types. Dissected cells were stained, expanded and dried according to the SPEx protocol. Images are not to scale (magnification of the objective used for dissection is indicated). Scale bar, 100 µm. **(F)** UpSet plot showing shared and unique proteins identified across the different regions of interest (ROIs) shown in (E). **(G)** Principal component analysis (PCA) of proteomics samples from the same ROIs shown in (E).

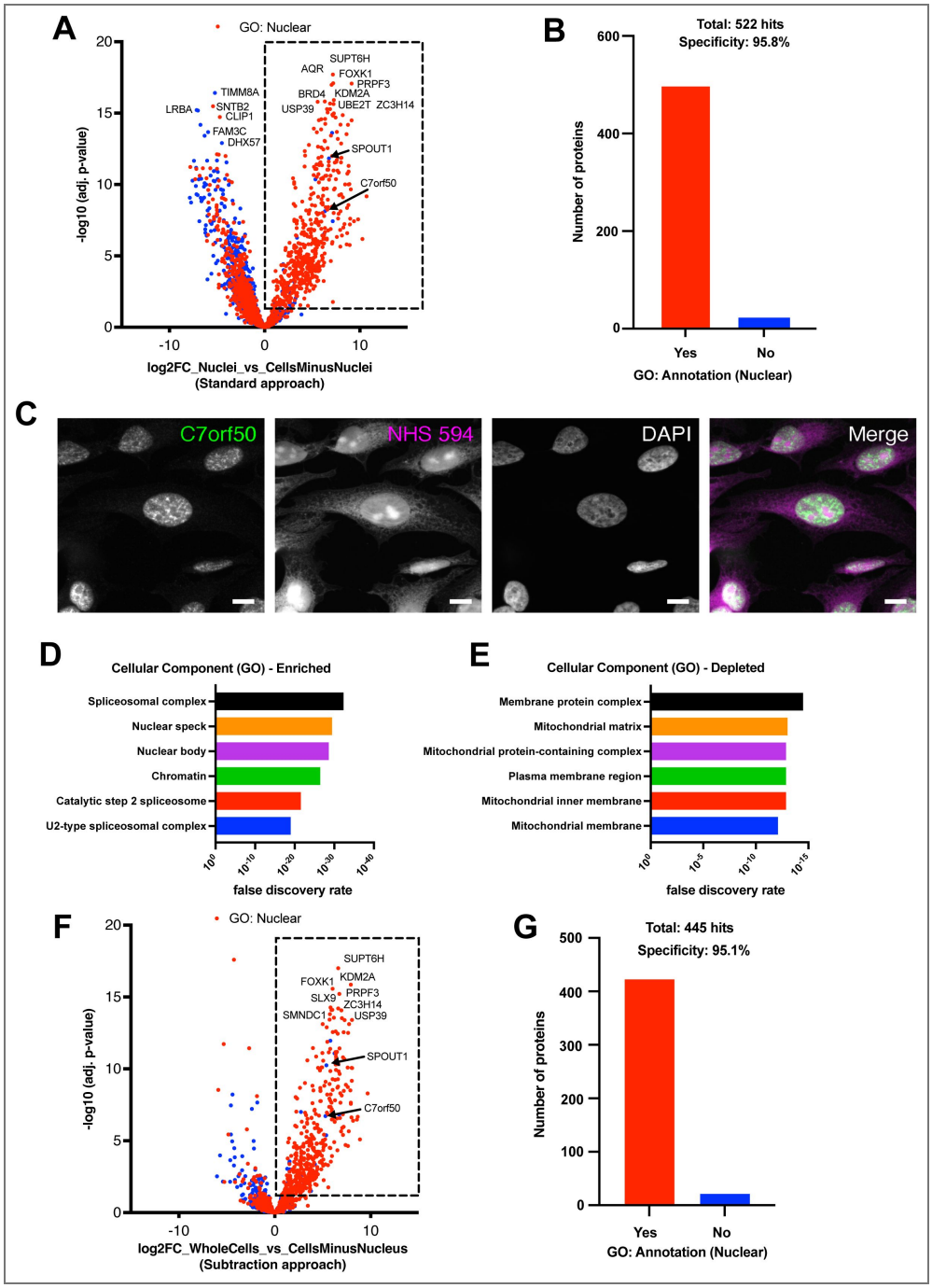

Figure 3. Application of SPEx to the nucleus

(A) Volcano plot of pairwise proteomic comparison between Nuclei and CellsMinusNuclei samples. The dotted square indicates proteins significantly enriched in the nucleus (adjusted $P < 0.05$, $\log_2FC > 0$). Red dots represent proteins annotated as nuclear according to Gene Ontology (GO). FC, fold change. **(B)** Number of proteins significantly enriched in the nucleus in (A) (dotted square) that are annotated as nuclear (Yes) or not nuclear (No) according to GO. **(C)** HeLa cells immunostained for C7orf50 and stained with DAPI and NHS 594. DAPI is omitted from the merged image for clarity. Scale bar, 10 µm. **(D)** Functional enrichment analysis of all proteins shown in (A) for cellular components using Gene Ontology (GO) via STRING (*string-db.org*). The six most significantly enriched terms (ranked by FDR) are shown. All significant terms (FDR < 1%) are listed in Supplementary Table S7. **(E)** Same analysis as in (D), showing the six most significantly depleted GO terms. **(F)** Volcano plot of pairwise proteomic comparison between WholeCells and CellsMinusNucleus samples. The dotted square indicates proteins significantly enriched in WholeCells (adjusted $P < 0.05$, $\log_2FC > 0$). Red dots represent proteins annotated as nuclear according to GO. **(G)** Same analysis as in (B) for proteins significantly enriched in WholeCells (F, dotted square).

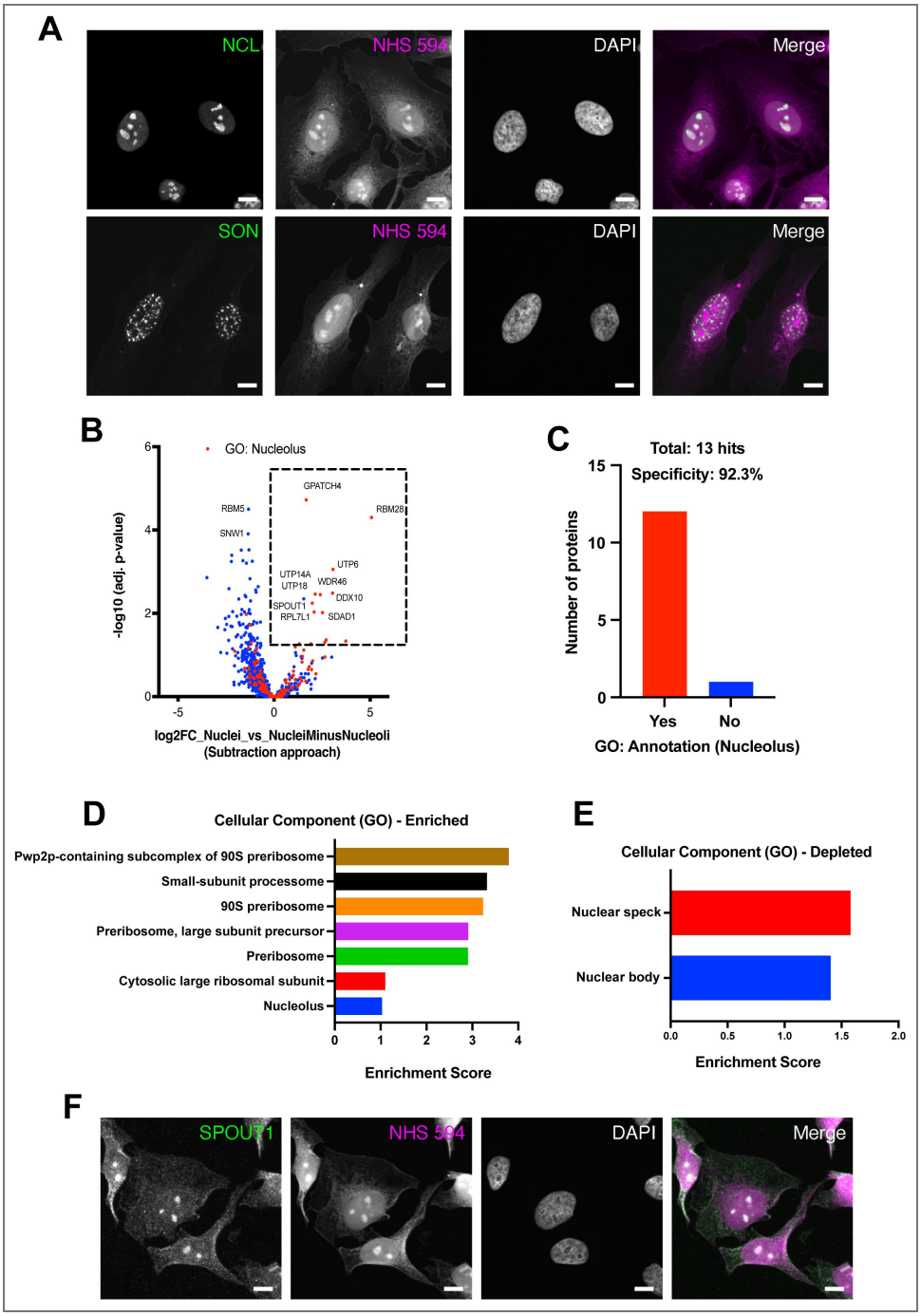

Figure 4. Application of SPEx to nucleoli

(A) HeLa cells immunostained for NCL (nucleolar marker) or SON (nuclear speckle marker) and stained with DAPI and NHS 594. DAPI is omitted from the merged image for clarity. Scale bar, 10 µm. **(B)** Volcano plot of pairwise proteomic comparison between Nuclei and NucleiMinusNucleoli samples. The dotted square indicates proteins significantly enriched in nuclei (adjusted $P < 0.05$, $\log_2FC > 0$). Red dots represent proteins annotated to localize to the nucleolus according to Gene Ontology (GO). **(C)** Number of proteins significantly enriched in (B) that are annotated as nucleolar (Yes) or not (No) according to GO. **(D)** Functional enrichment analysis of all quantified proteins shown in (B) for cellular components using Gene Ontology (GO) via STRING (*string-db.org*). The seven most enriched significant terms (ranked by enrichment score) are shown. All significant terms (FDR < 1%) are listed in Supplementary Table S11. **(E)** Same analysis as in (D), showing the two significantly depleted GO terms. **(F)** HeLa cells immunostained for SPOUT1 and stained with DAPI and NHS 594. DAPI is omitted from the merged image for clarity. Scale bar, 10 µm.

the nucleus. To take this analysis a step further, we wanted to assess the specificity of detection of non-nuclear proteins in the depleted fraction. Therefore, we determined the proportion of proteins with mitochondrial, but absent from the list of nuclear annotated proteins. Overall, 164 proteins annotated 'mitochondrial' were found in our dataset and all but one of them were reduced in abundance in our nuclear sample (Figure S1C). Only SPOUT1 was found to be significantly enriched in the nuclear fraction, but this protein is actually not a mitochondrial protein and found to be nuclear (Figure 4F). Taken together, the SPEx method cannot only be used to quantitatively identify proteins specifically enriched in an organelle, but also proteins, which concentrations are reduced in an organelle. The quantitative aspect of our approach, makes it highly suitable for the analysis of changes in protein localization under different conditions.

Encouraged by these results and as another test of the quantitative aspect of our method, we asked whether we could determine the proteome by subtraction (Figure S1D). Specifically, we wondered, if we compare the proteome of entire cells (WholeCells) to the one of cells from which we cut out the nucleus (CellsMinusNucleus), would we still be able to retrieve the nuclear proteome? We thought this might be feasible because the samples were well-separated in the PCA (Figure 2G). To our delight, this approach likewise showed a high enrichment of nuclear proteins (Figure 3F and G), achieving almost the same high specificity (95%) and coverage (423 nuclear proteins) compared to using the standard approach on the nuclei samples (Figure 3A and 3B). Moreover, the high overlap of the significantly enriched proteins confirmed the high specificity achieved with either comparison. In fact, the about 400 proteins, which were common between the two analyses (Figure S1E) showed an extraordinary nuclear specificity of 98% (Figure S1F). Thus, the subtraction method can also be used to reliably identify the proteome of a compartment, without analyzing the compartment itself. Moreover, combining the two quantitative analyses can be used to further boost the specificity of the SPEx method.

To further assess the specificity and performance of our method, we next compared it to previously published large subcellular datasets, based on either subcellular fractionation followed by proteome profiling (Geladaki et al., 2019; Orre et al., 2019) or native immunoprecipitation proteomics of organelles (Hein et al., 2025) (Supplementary tables 8 to 10). While the other methods could overall identify more proteins in their nuclear fractions (Figure S1F), SPEx achieved the highest specificity of all datasets (Figure S1G).

Taken together, SPEx is a new method to identify reliably and with high specificity nuclear proteins from low input samples. SPEx serves also as a discovery tool as we identified unannotated nuclear proteins. Moreover, our method is quantitative and efficiently determined proteins that were depleted or absent from nuclei.

SPEx identifies the nucleolar proteome

To test whether SPEx also allows the determination of the proteome of much smaller structures within the cell, we aimed to investigate the proteome of nucleoli. Targeting nucleoli bears another challenge in that nucleoli are membraneless organelles and many components are constantly exchanging between the nucleoplasm and the nucleoli, unlike when targeting a membrane-bounded organelle. Furthermore, the biochemical purification of membraneless organelles is challenging, and hence, the composition of the nucleolus is mostly based on imaging data or on GO annotation trained algorithm (Hein et al., 2025 Cell).

First, we aimed to confirm that the NHS ester-stained structures in the nucleus are indeed nucleoli. Therefore, we stained cells for nucleolin (NCL), an established nucleolar marker, or SON, which marks nuclear speckles (Hondele et al., 2019; Su et al., 2013). Indeed, NHS ester marks specifically nucleoli and not nuclear speckles (Figure 4A). We therefore cut out 100 nucleoli and subsequently the corresponding nuclei without nucleoli (NucleiMinusNucleoli) and compared their proteomes (Figure S2A). We detect about 300 proteins, of which according to GO only 11% were annotated to be nucleolar localized (Figure S2B). One reason could be that most nucleolar protein shuttle between the nucleoli and the nucleoplasm, and therefore their abundance could be rather similar in the nucleoplasm and the nucleoli, while their concentration could be still higher in the nucleoli. Moreover, the volume of the nucleus is much bigger than the combined volume of

the nucleoli, which we excised, making quantitative comparison more challenging. To circumvent these problems, we applied the subtraction method to detect which proteins are reduced in the NucleiMinusNucleoli samples compared to the Nuclei samples. Using this method, we increased the specificity from 10.8% to 92.3%, at the expense of number of specific hits (Figure 4B). Still, from the 13 significantly enriched proteins all but one, SPOUT1, were annotated by GO to be nucleolar (Figure 4C). We have already identified SPOUT1 as a novel nuclear protein above (Figure 3A). Our nucleoli analysis suggested that SPOUT1 is actually a nucleolar protein that we could confirm by immunofluorescence (Figure 4D). Moreover, functional enrichment analysis showed that proteins associated with the 90S pre-ribosome, which are specifically localized in the nucleolus, were most enriched (Figure 4D and Supplementary table 11). Thus, despite this high stringency, we were still able to identify a novel component of the nucleolus. It is worthwhile noting that while the subtraction method strongly reduced the number of potential false positive, the most significant enriched proteins were also found by the standard method in which we compared Nucleoli to NucleiMinusNucleoli (Figure 4B and S2A), indicating that nucleoli proteins were also enriched in the excised nucleoli fraction. Moreover, the standard method might at times be more useful as a discovery tool. Nevertheless, we successfully identified proteins of the membraneless nucleolus using expanded *in situ* laser-dissected samples.

The nucleolus is not the only membraneless organelle in the nucleus. Like nucleoli, those other organelles, such as nuclear speckles, have a high local concentration of their protein components, but these proteins are likewise present in the nucleoplasm, and both pools are constantly exchanging. However, exchange between constituents of nucleoli with constituents of other nuclear membraneless organelles is expected to be limited. As a further test for specificity, we asked whether we could detect components of the other nuclear membraneless organelles in the fraction that is depleted or absent from nucleoli. In both, the standard and the subtraction method, RBM5 and SNW1 were very significantly depleted from the nucleoli fraction (Figure 4B and S2A). RBM5 is a component of the spliceosome A complex and SNW1 a component of the minor spliceosome. The spliceosome has been shown to be located in nuclear speckles (Bhat et al., 2024) and, according to protein atlas (Figures S2C and S2D), RBM5 and SNW1 are indeed located in nuclear speckles and absent from the nucleolus. Moreover, functional enrichment analysis revealed that nuclear speckle and nuclear body proteins were significantly depleted from our nucleolar fraction (Figure 4E and Supplementary table 11). Therefore, also for the nucleolus, we were able to determine proteins that were specifically depleted/absent from nucleoli in an environment, which is guided by protein diffusion.

To date, only few subcellular proteome studies assigned nucleolar locations to proteins, because membraneless organelles are notoriously difficult to purify (Orre et al., 2019)(Supplementary table 8). By contrast, SPEx allows isolation and collection of organelles directly from cells and is therefore ideally suited for the enrichment and analysis of membraneless organelles. This is nicely demonstrated by the higher specificity for nucleolar proteins obtained by SPEx (>90%) compared to classical density gradient centrifugation with only around 50% (Orre et al., 2019) (Figure S2E and S2F).

Taken together, SPEx not only allowed us to detect nucleolar proteins with very high specificity, we also identified an unannotated nucleolar protein. Moreover, compared to other available methods, SPEx demonstrated a higher specificity assignment of proteins for a membraneless organelle, like the nucleolus.

Golgi proteins are identified with high specificity using SPEx

Finally, we used SPEx to determine the proteome of the Golgi. The Golgi is a central sorting station for proteins and lipids and which is responsible for post-translational modifications such as glycosylation. It is a highly dynamic structure, and transport through the Golgi and the dynamics of Golgi cisternae are still a matter of debate. To address these issues, it would be desirable to have a method, which could capture the Golgi in different states. Recently developed immunoprecipitation methods have tackled this challenge (Fasimoye et al., 2023), however, because of a few time-consuming purification steps, important transient molecular interactions

might still be lost. SPEx, on the other hand, allows direct isolation of organelles from fixed cells with preserved molecular composition and should therefore be well suited for the analysis of this dynamic organelle.

To test this exciting possibility, we excised 35 Golgis and compared them to the corresponding cells without Golgi (CellsMinusGolgi) (Figure 5A). We identified 356 significantly enriched proteins in the Golgi samples, 288 (80.9%) were GO annotated with Golgi or extracellular localization (Figure 5B). The later class most likely represents cargo traveling through the Golgi. Among the enriched proteins were many proteins related to glycosylation such as GALNT1,2 and 7 (Figure 5A). We also detected a number of Golgins (GOLGA2-4); GOLGA2 (GM130) was our Golgi marker. Moreover, numerous trafficking-related Golgi proteins such as the SNARE receptor GOSR1, the COG tethering proteins and the coatomer complex, which is the coat of COPI vesicles, were highly enriched in the Golgi fraction. The method was sensitive enough to also to detect the Golgi Rab, Rab6A (Figure 5A). In contrast, endosomal proteins such as SNX2, CHMP4A and B or EHD2 were depleted as well the components of the adaptor complex for clathrin-mediated endocytosis such as AP2A2 or the plasma membrane exocyst tether EXOC8 (Figure 5A). Interestingly, we also observed depletion of the ARP2/3 complex from the Golgi fraction. Notably, the comparison of WholeCells to CellsMinusGolgi also enriched for Golgi proteins (Figure S3A), but with a somewhat lower specificity (Figure S3B), similar to what we observed for the analysis of the nucleus (WholeCells-CellsMinusNucleus). Functional enrichment analysis confirmed the high specificity of Golgi proteins in our SPEx results. The most enriched cellular components were all associated to the Golgi (Figure 5C and Supplementary table 12), whereas the most depleted protein groups were all assigned to the nucleus (Figure 5D). This result may not be very surprising, because the nucleus has the highest protein content and there is essentially no overlap with Golgi proteins.

Our analysis also identified proteins that were not annotated to be Golgi localized previously. We selected again one candidate for confirmation, KIAA2013, (Figure 5A) and determined the subcellular localization using immunofluorescence (Figure 5E). We confirmed that KIAA2013 is indeed Golgi localized and, thus, again we were able to assign a new location to a protein. Compared to previously published large scale datasets (Fasimoye et al., 2023; Geladaki et al., 2019; Hein et al., 2025; Orre et al., 2019; Schessner et al., 2023) (Supplementary tables 8-10 and 13-14), SPEx achieved comparable results with a high proteome coverage (Figure 5F) and similar specificity (Figure 5G).

Discussion

Here, we report the development of SPEx as a method for *in situ* subcellular spatial proteomics at a single micrometer resolution. To achieve this, we combined expansion microscopy with laser dissection and LC-MS/MS. SPEx requires low sample input, is low cost and adaptable to membrane-bounded and membraneless organelles. Depending on the size of the organelles, SPEx can be readily used for subcompartments of organelles.

To establish the protocol, we took advantage of the well-known TREx protocol, which allows up to 10x expansion without the need for any specialized equipment or procedures (Damstra et al., 2022). Drying the samples onto a PPS-membrane still maintained an about 7x linear expansion in X and Y, resulting in almost 50x increase of surface area. This increase enlarges the subcellular regions to an extent that they can be easily excised by laser microdissection. To demonstrate the general applicability of SPEx we chose a diverse set of targets in this study: the nucleus, the nucleolus and the Golgi. Those targets differ in size, shape, labeling method required for visualization (dyes and IF) and architecture (membrane-bound and membraneless organelles). We also show that surprisingly only a couple of dozens of organelles are required as sample input for LC-MS/MS. These inputs were sufficient to obtain good coverage and high specificity. Importantly, we detected not only predicted or previously known components of these well-studied organelles, we also identified novel proteins residing in the nucleus, the nucleolus and the Golgi with high specificity. Of note, membraneless organelles are inherently difficult to purify. SPEx overcomes this problem by eliminating the need of biochemical enrichment procedures. Moreover, SPEx

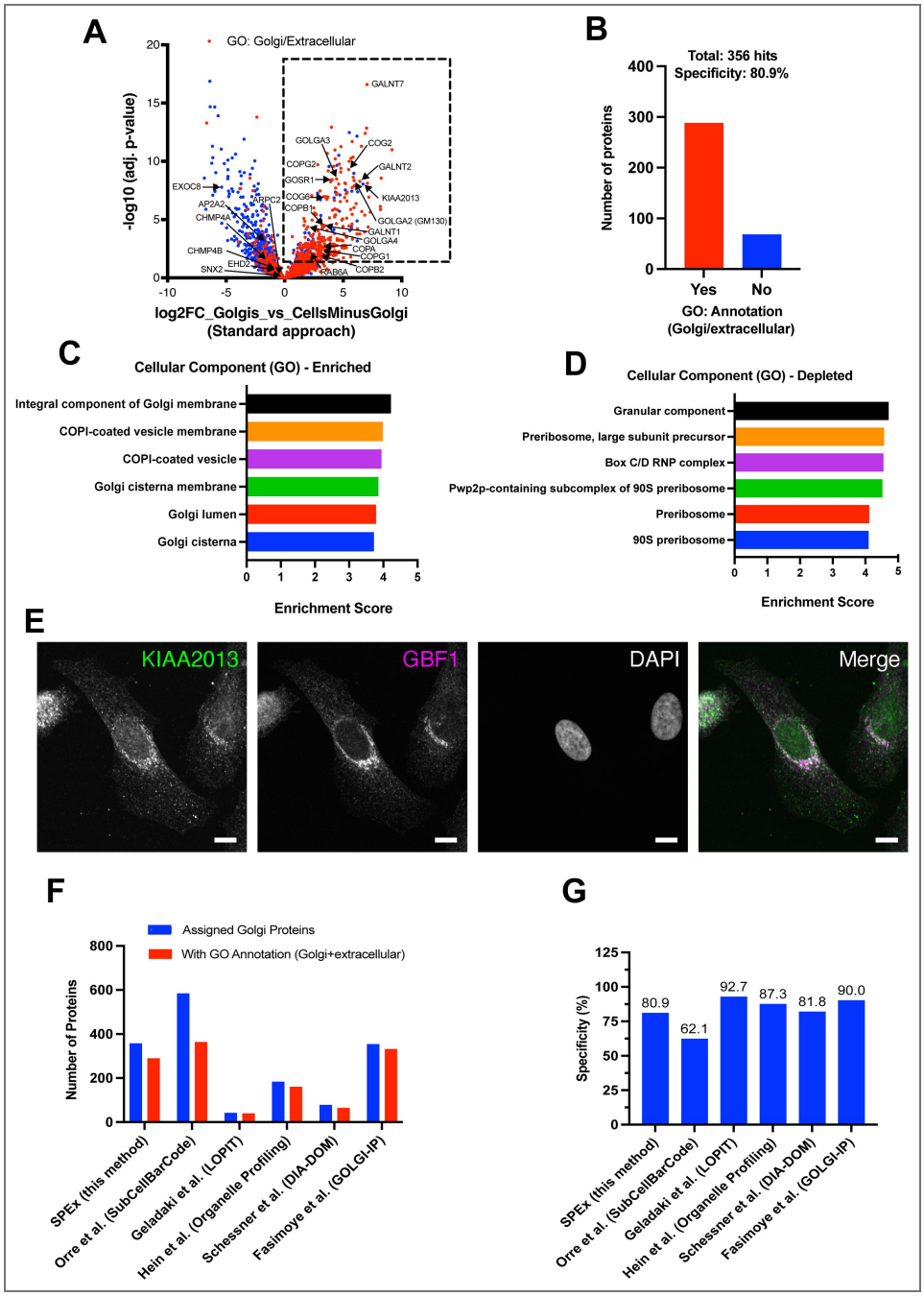

Figure 5. Application of SPEx to the Golgi

(A) Volcano plot of pairwise proteomic comparison between Golgis and CellsMinusGolgi. The dotted square indicates proteins significantly enriched (adjusted $P < 0.05$, $\log_2FC > 0$) in the Golgi. Red dots represent proteins annotated to localize to the Golgi and/or to be extracellular according to GO. **(B)** Number of proteins significantly enriched in the Golgi in (A) that are annotated as Golgi and/or extracellular (Yes) or not (No) according to GO. **(C)** Functional enrichment analysis of all quantified proteins shown in (A) for cellular components using Gene Ontology (GO) via STRING (*string-db.org*). The six most enriched terms (ranked by enrichment score, FDR < 1%) are shown. All significant terms (FDR < 1%) are listed in Supplementary Table S12. **(D)** Same analysis as in (C), showing the six most depleted GO terms. **(E)** HeLa cells immunostained with antibodies for KIAA2013 and GBF1 (Golgi marker) and stained with DAPI. DAPI is not shown in the merged image for clarity. Scale bar, 10 µm. **(F)** Bar plot comparing the number of proteins assigned to the Golgi (blue) in our SPEx dataset (this study, A) with other published spatial proteomics datasets (Fasimoye et al., 2023; Geladaki et al., 2019; Hein et al., 2025; Orre et al., 2019; Schessner et al., 2023). Proteins overlapping with GO Golgi/extracellular annotations are shown in red. **(G)** Specificity of GO Golgi/extracellular annotation in the different proteomics datasets, determined from (F).

compares favorably to other specialized enrichment procedures. We compared the coverage and specificity of SPEx to a number of currently available other spatial proteomics methods, based on either subcellular fractionation followed by proteome profiling (Geladaki et al., 2019; Orre et al., 2019; Schessner et al., 2023) or native immunoprecipitation proteomics of organelles (Fasimoye et al., 2023; Hein et al., 2025). When applied to the nucleus or nucleoli, SPEx showed either better coverage or better specificity than currently available methods. When we employed SPEx to the Golgi, we were able to obtain coverage and specificity comparable to currently available methods including a specific Golgi-IP (Fasimoye et al., 2023). Another great advantage of SPEx is that it does not rely on transfection of fusion proteins, changes in the media or other manipulations. Whatever method can be used to visualize the region or structure of interest is sufficient to perform SPEx. We used the same overall protocol for the sample preparation and the analysis of the nucleus, nucleoli and Golgi, indicating that not much, if any, tinkering has to be done to perform a successful SPEx experiment. Sampling of different structures from the same preparation (e.g. whole cells, nucleus, cells without nucleus, nucleoli, nuclei without nucleoli) abolishes the need of separate sample preparations for different targets and controls.

Our data show that SPEx data can be analyzed efficiently in two different ways. The standard approach is to isolate structures of interest and compare their proteome to the one of cells or subcellular compartments from which the structures were removed (control). The other, useful option is the subtraction approach, which is an indirect measure, but still very powerful. In this case, the structure of interest is cut out. The analysis, however, is performed on the cell/organelle from which the structure of interest has been excised and compared to the cell/organelle in which the structure is still present. Both approaches yield comparable results in our test cases. The standard approach is well-suited for most questions and approaches, and also for the discovery of transiently interacting or low abundant proteins. The subtraction method detects proteins that were lost from one sample, and thereby is highly specific and gives less false positives. This approach might be particular useful when venturing into the unknown and markers of a compartment or domain should be identified. Even though we obtain about 7x fold expansion of our dried samples, this magnification might not be sufficient to cut out and analyze organellar subcompartments such as membrane contact sites. In those cases, eliminating these structures from the sample might provide the specificity to identify key proteins of these structures.

We have great resolution in X-Y direction (50x surface area increase), however no resolution in Z. We were, therefore, initially worried about potential contamination and false positive detection of proteins. To our delight, it turned out that this was not a big problem. Proteins present on an organelle will still be enriched in the sample, while the level of the cytoplasmic or plasma membrane proteins will remain at the same levels in the sample and the control, and hence these proteins are not enriched in the organellar fraction. Even though, we may also cut out other organelles or pieces thereof, this will likewise happen in the control. Our data show that the lack of resolution in Z is a much lesser problem than initially anticipated.

We think that SPEx holds great potential to answer spatial proteomics questions that were hard to tackle as of yet. A great strength of SPEx is that the experimentalist specifically selects the (sub) compartments for the analysis, which is in marked difference to proximity labeling techniques. SPEx could, thus, be used to quantitatively determine the composition of fragmented versus fused mitochondria or between tubular and sheet endoplasmic reticulum in the same cell. We foresee also the use to detect other organellar subcompartments. Moreover, compared to other spatial proteomics methods currently used, SPEx requires very little prior knowledge and no genetic manipulation of the studied system. Visualizing an organelle or compartment just by morphology would be sufficient for SPEx. Thus, even structures for which no antibodies are available could potentially be analyzed using SPEx. This, together with the fact that the TREx expansion method has been shown to be widely applicable to different cell types and tissues (Damstra et al., 2022), leads us to believe that SPEx could be a valuable tool to perform spatial proteomics on hard to transfect cells, tissues and non-model organisms were genetic manipulation and/or antibody staining remains highly challenging.

Another potential application of SPEx lies in studying cell to cell heterogeneity, because SPEx allows to not only perform spatial proteomics on specific organelles, but also allows researchers to select in which cells these organelles should be isolated. This would allow for comparative studies, where the proteome of specific organelles in morphologically different cells in the same dish (e.g. dividing vs non-dividing or responders vs non-responders in drug treatment) could be determined. This remains challenging with conventional methods, due to the generation of lysates from many cells prior to enrichment. Therefore, the analysis on the single cell level remains difficult with these methods. Gratifyingly, SPEx does allow these types of analyses.

It is conceivable that the SPEx approach could be used beyond the context of spatial proteomics. It is conceivable that in the future, this approach could be coupled to downstream lipidomics allowing to study the membrane composition of different organelles/domains in the cell. Possibly, the same workflow could also be used to perform RNA/DNA sequencing to determine the RNA content of condensates or the DNA content of specific nuclear regions.

In summary, by combining ExM, LMD and low input LC-MS, SPEx offers a novel approach to subcellular spatial proteomics. The low sample requirements and flexible nature of the SPEx method make it a useful approach to tackle spatial proteomics questions that were previously hard to investigate and required the development of highly specialized methods.

Material and methods

Reagent type (species) or resource	Designation	Source or reference	Identifiers	Additional information
Antibody	NCL (Mouse Monoclonal)	Abcam	ab136649	Dilution (1:500)
Antibody	SON (Rabbit Polyclonal)	GeneTex	GTX123778	Dilution (1:5000)
Antibody	GOLGA2/GM130 (Rabbit Polyclonal)	Proteintech	11308-1-AP	Dilution (1:200)
Antibody	SPOUT1 (Rabbit Polyclonal)	Atlas Antibodies	HPA022990	Dilution (1:50)
Antibody	KIAA2013	Atlas antibodies	HPA060536	Dilution (1:10)
Antibody	GBF1 (Mouse Monoclonal)	BD Biosciences	AB_399487	Dilution (1:200)
Antibody	C7ORF50	Atlas Antibodies	HPA052281	Dilution (1:65)
Antibody	Rabbit IgG Alexa Fluor 594 (Goat Polyclonal)	ThermoFisher	A-11012	Dilution (1:200) for ExM, Dilution (1:500) for IF
Antibody	Mouse IgG Alexa Fluor 594 (Goat Polyclonal)	ThermoFisher	A-11005	Dilution (1:500)
Antibody	Rabbit IgG Alexa Fluor 488 (Goat Polyclonal)	ThermoFisher	A-11008	Dilution (1:500)
Antibody	Mouse IgG Alexa Fluor 488 (Goat Polyclonal)	ThermoFisher	A-11001	Dilution (1:500)
Cell line (homo sapiens)	HeLa CCL2	Gift from Dr. Martin Spiess		

Key resource table

Cell culture

HeLa cells were cultured at 37°C and 5% CO_2 in growth media (DMEM high-glucose medium (Sigma-Aldrich, D57969) with 10% FCS (Biowest, S1810), 1% penicillin–streptomycin (Sigma-Aldrich, P4333), 1 mM sodium pyruvate (Sigma-Aldrich, S8636) and 2 mM L-Glutamine (Gibco, 25030-024)). Cells were regularly tested for mycoplasma using a Mycoplasma PCR detection kit (Applied Biological Materials, G238).

Fixation and immunofluorescence

50,000 HeLa Cells were seeded on sterile 13 mm glass coverslips (VWR, 631-0150) in a 24-well plate (Sarstedt, 83.3922). Cells were incubated at 37°C, 5% CO_2 O/N, washed once in PBS (Gibco, 20012-019) and fixed in 3% PFA (Sigma, F8775-500ML) in PBS for 10 minutes. Cells were washed 3x in PBS and permeabilized with 0.1% Triton (Sigma, T8787-50ML) in PBS for 10 minutes. After permeabilization, cells were washed 3x in PBS and incubated in blocking solution (1% BSA (Sigma-Aldrich, A9647-100G) in PBS) for 30 minutes. Coverslips were transferred to a wet chamber and incubated for 1 hour in primary antibody (for dilutions see resource table) in blocking solution. Coverslips were washed 3x in PBS and incubated for 30 minutes in secondary antibody in blocking solution (for dilutions see resource table). Cells were washed 3x in PBS. Cells were incubated with 1 µg/ml DAPI (Sigma-Aldrich, D9542-10MG), and 0.2 µg/ml NHS Atto 594 (Sigma-Aldrich, 08741-1MG-F) or NHS Atto 488 (Sigma, 41698-1MG-F), where applicable, in PBS for 1 hour at 37 °C. After washing 3x in PBS for 5 minutes, coverslips were mounted on fluoromount G (SouthernBiotech, 0100-01) and left to settle overnight in the dark. Unless mentioned otherwise, all steps were performed at room temperature (RT). Confocal images were acquired with Evident/Olympus Fluoview FV3000 laser scanning system equipped with solid-state lasers and a galvanometer scanner using an UPLSAPO 60×/1.30 objective with silicone oil (Evident/Olympus, Z81114) and FV31S-SW software.

SPEx Workflow

Fixation and immunofluorescence for SPEx

Sterile 13 mm coverslips were prepared in a 24-well plate. Coverslips were coated by incubating them in coating solution (Fibronectin bovine plasma (Sigma-Aldrich, F1141-5MG) 1:200 in ddH_2O) for 90 minutes at RT. The coating solution was aspirated and the coverslip were air dried for 20 minutes and washed once in PBS. 20,000 HeLa Cells were seeded in DMEM (low confluency (~30-40%) is crucial for optimal expansion) and incubated at 37°C, 5% CO_2 O/N.

Cells were washed once in PBS and fixed for 10 minutes at 37°C with pre-warmed fixation mix (4% PFA in PBS). Cells were washed 2x in PBS. If no IF was performed cells were permeabilized for 10 minutes in 0.1% Triton in PBS and subsequently washed 3x in PBS (for non-IF samples proceed to “TREx expansion”). For IF, cells were blocked for 1 hour in blocking solution (3% BSA, 0.1% Triton in PBS) with gentle rocking. Next, cells were incubated with primary antibody (for dilutions see resource table) in blocking solution for 3 hours with gentle rocking. Cells were washed 3x 5 minutes in PBS with gentle rocking and incubated with secondary antibody (for dilutions see resource table) in blocking buffer O/N at 4°C with gentle rocking. Cells were washed 3× 10 minutes in PBS with gentle rocking. Unless mentioned otherwise, all steps were performed at RT. Adapted from (Damstra et al., 2022).

TREx Expansion

Prior to the expansion, gelation chambers and gelation solution were prepared as follows:

- Gelation chamber: Two holes of 3-4 mm diameter (spaced apart by ~3mm) were punched into a microscopy-slide-sized piece of parafilm (Parafilm, PM-996) using a tissue puncher. The parafilm was then placed on a glass microscopy slide (Epredia, AG00008032E01MNZ20) (paper side up) and adhered by repeatedly streaking over it and finally removing the paper on the parafilm.
- Gelation solution: The base of the gelation solution (1.1 M sodium acrylate (Sigma, 408220-

25G), 2 M acrylamide (Sigma, A4058-100ML), 0.005% Bis (Sigma, M1533-25ML), 1x PBS (Thermo Fischer, 70011044)) was mixed, aliquoted and stored at –20°C. Before gelation aliquots were thawed to RT (prevents incomplete sodium acrylate dissolution) and then placed on ice. Right before use 0.15% TEMED (Sigma, S7653-250G) and 0.15% APS (Sigma, A3678-25g) were added, the solution was mixed thoroughly and placed back on ice immediately.

Anchoring was performed by incubating cells for 1 hour in 0.05 mg/ml AcX (Invitrogen, A20770) in PBS. Cells were washed once in PBS. The coverslip was rinsed once in gelation solution and 4 µL of gelation solution was added to each hole of the gelation chamber. The coverslip was placed on the gelation chamber with the cells facing down and a second 18 mm square coverslip was put on top. Clamps were used to press down the coverslip during gelation to obtain thinner gels. The assembled gelation chamber was incubated for 1 hour at 37°C. Gels were removed from the gelation chamber into 2 mL Eppendorf tubes and rinsed twice in PBS. Non-proteolytic disruption was performed by incubating the gels in disruption buffer (5% SDS (Sigma, 436143-25G), 200 mM NaCl (Sigma, S7279-25G), 50 mM Tris pH 8 (Invitrogen, AM9855G)) O/N at 95°C on a heating block. After disruption, gels were rinsed once in 0.4 M NaCl, followed by two 30 minutes washes in PBS with gentle rocking. Gels were stained with 20 µg/ml DAPI and 20 µg/ml NHS-Atto 488 or NHS-Atto 594 in PBS for 1 hour at 37°C. After staining, gels were rinsed once in PBS and transferred to a container with large volumes of Milli-Q water. Gels were expanded for 2x 30 minutes in MilliQ-water with gentle rocking. The water was exchanged again, and gels were left to expand O/N with gentle rocking. Unless mentioned otherwise, all steps were performed at RT. Adapted from (Damstra et al., 2022). The hydrated gels were transferred into a 30 mm imaging dish (Ibidi, 81156) and imaged on a CSU-W1 spinning disk confocal (Evident/Olympus), mounted on a IX83 stand and equipped with diode lasers and Hamamatsu ORCA-Fusion sCMOS cameras. The images were acquired with a 30x UPL S APO 1.05 NA silicon objective (Olympus) and cellSens Dimension software (Evident Scientific, version 4.3.1).

Drying of gels onto membrane slides

Fully expanded gels were trimmed with a scalpel and placed on a steel frame slide with PPS-membrane (Leica, 11600294). Excess water was removed with a tissue paper. The slide was incubated at 37°C for 3 hours to dry the gels. Membrane slides were stored at 4°C in a desiccator in the dark until laser dissection.

Widefield images of dried samples (and corresponding non-expanded controls) were captured using the Zeiss Imager.M2 with an EC Plan-NEOFLUAR 20x/0.5 (air) objective and ZEISS ZEN 3.9 Software.

Laser Microdissection

Laser Microdissection was performed using a LMD7 (Leica Microsystems) equipped with an Ultra LMT350 stage, and a 12-bit K3M monochrome camera. A 349 nm diode-pumped solid-state laser was used for microdissection, and the samples were cut using with a HC PL FLUOTAR 10x/0,30, a HC PL FLUOTAR L 40x/0.60 CORR XT or a HC PL FLUOTAR L 63x/0,70 CORR XT (Leica, 11506505, 11506208 or 11506222 respectively) and samples were collected into a low bind 96-well plate (Eppendorf, EP0030129512). In the Leica LMD software (version 8.5), ROIs were outlined using the drawing tool and collected using the “Middle Pulse” mode; objectives used and number of ROIs collected were adjusted for different sample types (Supplementary table 3). Images pre– or post-cuts were done with either a HC PL FLUOTAR 10x/0,30, a HC PL FLUOTAR L 40x/0.60 CORR XT or a HC PL FLUOTAR L 63x/0,70 CORR XT.

Sample preparation for LC-MS

To avoid sample loss, all buffers were added to the side of the well, followed by a quick spin. Whenever the sample was transferred, low-bind tips were used. After collection 7µL of lysis buffer (100 mM tetra-ethyl ammonium bicarbonate (TEAB) (Supelco, 18597), 0.02% n-dodecyl-ß-maltoside (DDM) (Sigma, D4641), 10 mM tris(2-carboxyethyl)phosphine (TCEP) (Sigma-Aldrich, 626547), 15 mM 2-chloroacetamidecan (CAA) (Sigma, C0267), were added to the sample in the low bind 96-well

plate. The sample was heated to 95°C for 1 hour in a thermal cycler. After cooling of the sample to RT, 1 µL of digestion buffer (60% acetonitrile (ACN) (EGT Chemie AG, RC-ACNMS-2.5L), 100 mM TEAB) was added. Next, the sample was again heated to 75°C for 30 minutes in a thermal cycler. After cooling the sample to RT, 2 µL of trypsin solution (10 ng/µL Trypsin (Promega, V5113), 50 mM TEAB, 0.01% DDM) was added and the sample was incubated for 12 hours at 37°C. The reaction was stopped by adding 1 µL of 5% trifluoracetic acid (TFA) (Thermo Fisher, 28904), and the sample was dried in a speedvac (Labconco, centrivap).

Finally, the peptides were cleaned by solid phase extraction using EvoTip Pure stage tips (EVOSEP, EV2020). The dried samples were heated to 37°C, resuspended in 10 µL resuspension buffer (0.1% TFA) using sonication for 5 minutes in a waterbath. The sample were loaded onto EvoTips by centrifugation following the vendor's protocol. Peptides were eluted with 20 ul elution buffer (40% ACN, 0.1% formic acid (FA)) direclty into a low bind 96-well plate, dried under vacuum and stored at –20 °C until further use.

LC-MS analysis

Peptides were resuspended in 5 µL 0.1% formic acid and the whole sample used for LC–MS/MS analysis using a timsTOF Ultra 2 Mass Spectrometer (Bruker) fitted with a Vanquish Neo HPLC (Thermo Fisher Scientific). The column heater was set to 60°C. Peptides were resolved using a RP-HPLC column (100µm × 30cm) packed in-house with C18 resin (ReproSil Saphir 100 C18, 1.5 µm resin; Dr. Maisch GmbH) at a flow rate of 0.4 µL min^{-1} at 60°C. A linear gradient of buffer B (80% acetonitrile, 0.1% formic acid in water) ranging from 2% to 25% over 25 minutes and from 25% to 35% over 5 minutes was used for peptide separation. Buffer A was 0.1% formic acid in water. The mass spectrometer was operated in positive DIA-PASEF mode. MS spectra were acquired from 100 to 1700 m/z. For MS/MS, we used eight MS/MS ramps and 24 MS/MS windows covering a mass-to-charge ratio range of 400–1000 m/z. This resulted in 25 Th wide MS windows and an ion mobility range from 0.64 to 1.37 V –s/cm². The mass spectrometer was operated in normal sensitivity mode, expected cycle time was 0.95 seconds, accumulation and ramp time was set to 100 ms. The following source settings were applied: 1600V Capillary Voltage and 3 l/min Dry Gas flow at 200°C. The collision energy was linearly ramped between 20 eV at 0.6 V –s/cm² and 59 eV at 1.6 V –s/cm².

Data analysis

The acquired raw files were searched using SpectroNaut (Biognosys, Schlieren, Switzerland, v19.0, default settings) against a human database (consisting of 20,360 protein sequences downloaded from Uniprot on 2022/02/22) and 393 commonly observed contaminants using the following search criteria: full tryptic specificity was required (cleavage after lysine or arginine residues, unless followed by proline); 3 missed cleavages were allowed; carbamidomethylation (C) was set as fixed modification; oxidation (M), N-acetlyation (N-term) were applied as variable modifications. The raw quantitative data was further statically analyzed using ProteoFlux (v1.8.3, Mollet, D., & Schmidt, A. ProteoFlux (Version 1.8.5) [Computer software]. *https://doi.org/10.5281/zenodo.18640999*) and Prism (v10.3.1, GraphPad). ProteoFlux is an open-source and reproducible workflow for quantitative proteomics data analysis. Prior to quantification, precursor intensities were filtered based on run-level posterior error probability (PEP) and q-value thresholds (≤ 0.01), and very low-intensity signals (below a threshold of 2) were treated as left-censored measurements. Precursor-level intensities exported from Spectronaut were aggregated to peptide-level quantities and subsequently summarized to protein abundances using a simple summarization-based approach, followed by median-based sample normalization and statistical analysis using linear models with empirical Bayes moderation. Exploratory data analysis included principal component analysis (PCA) of normalized protein intensities after left-censored missing value imputation and visualization of protein identification overlaps between conditions using UpSet plots. For differential proteome analysis, the raw quantitative data was filtered as follows: only proteins quantified with at least two unique peptides and in at least three replicates in one condition per contrast were considered. Subcellular location annotations (GO, cellular compartment) for all human proteins were downloaded from *www.uniprot.org* (06/02/2026) (Supplemental table 6). Functional enrichment analysis was carried out using

https://string-db.org/ (Szklarczyk et al., 2025) and the "Proteins with Values/Ranks" search scheme with default settings. Here, all protein accession numbers with their corresponding ratios of a specific contrast were imported. Only enriched terms with a Benjamini-Hochberg corrected FDR rate of 0.01% were considered (Supplemental table 7,11 and 12). The specificity of a specific contrast was determined by dividing the number significant protein hits (ratio >0, adjusted p-value <0.05) with correct subcellular GO annotation to all significant hits. Along these lines, the specificity of published methods was determined in the same way, using the list of all proteins assigned to the corresponding subcellular location as input.

Figure supplements

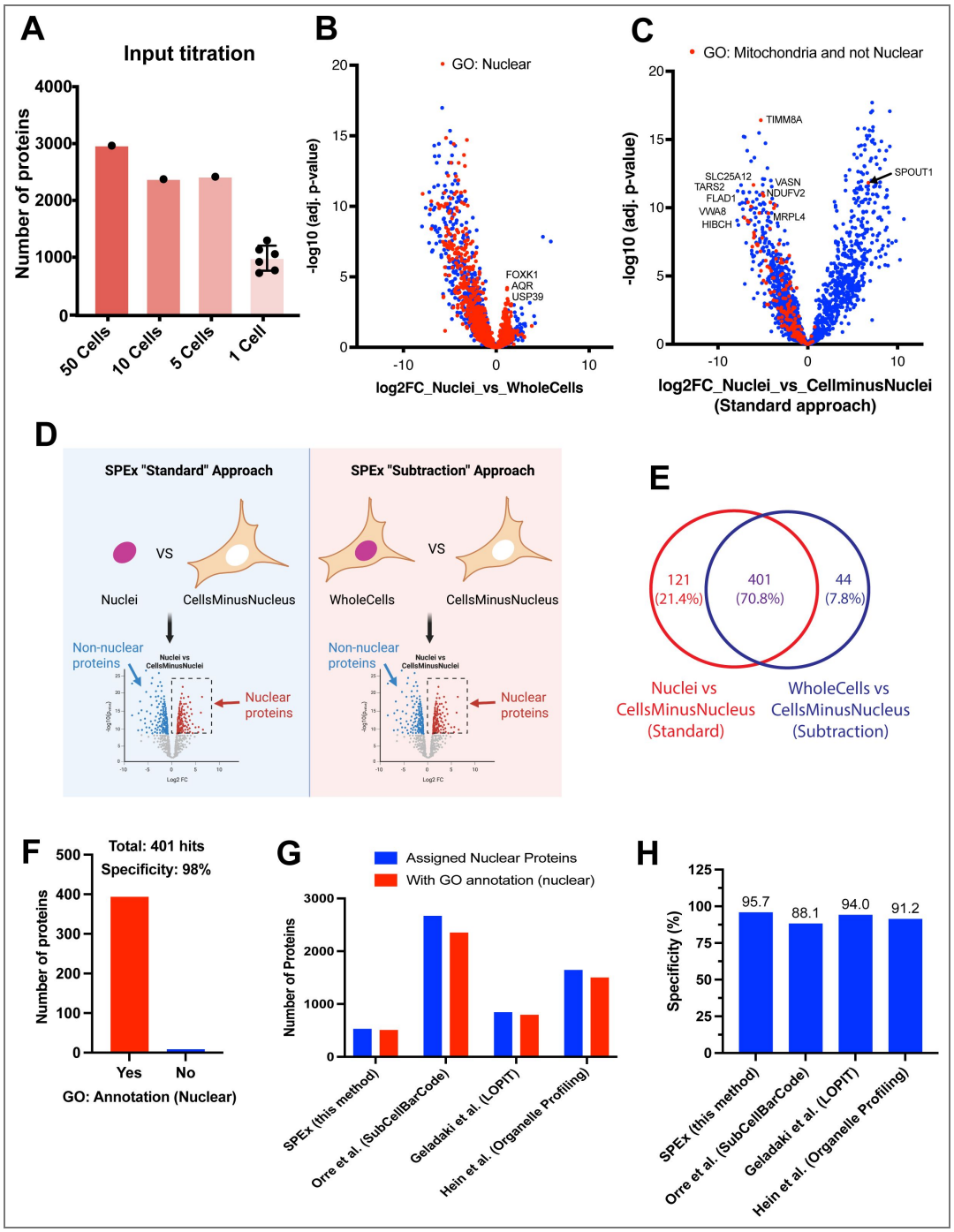

Figure S1. (**A**) Number of identified proteins for different input cell numbers. Data are mean ± SD: 50 cells: 2964; 10 cells: 2374; 5 cells: 2417; 1 cell: 982.5 ± 220.6 (n = 1 for 50, 10, and 5 cells; n = 6 for 1 cell; N = 1 experiment). **(B)** Volcano plot of pairwise proteomic comparison between nuclei and whole cells. Red dots represent proteins annotated as nuclear according to GO. **(C)** Volcano plot of pairwise proteomic comparison between nuclei and CellsMinusNuclei (same data as Figure 3A). Red dots represent proteins annotated as mitochondrial and not nuclear according to GO. **(D)** Schematic illustrating the SPEx "standard" approach and the SPEx "subtraction" approach. In the standard approach, the proteome of the organelle of interest (e.g., nuclei) is compared to the proteome of whole control cells from which the organelle was removed. In the subtraction approach, the proteome of a whole cell is compared to the proteome of a cell lacking the organelle of interest. In both approaches, proteins localized to the organelle of interest are enriched, and absent proteins are depleted. Created

in *BioRender.com*. **(E)** Venn diagram depicting the overlap of identified nuclear proteins between the standard SPEx (Figure 3A) and subtraction SPEx approach (Figure 3F). **(F)** Bar chart illustrating the number of proteins in the overlap shown in (E) with (Yes) and without (No) nuclear GO annotation. **(G)** Bar plot comparing the number of proteins assigned to the nucleus (blue) in our SPEx dataset (this study, A) with other published spatial proteomics datasets (Geladaki et al., 2019; Hein et al., 2025; Orre et al., 2019). Proteins overlapping with nuclear GO annotation are shown in red. **(H)** Specificity of nuclear GO annotation in the different proteomics datasets, determined from (G).

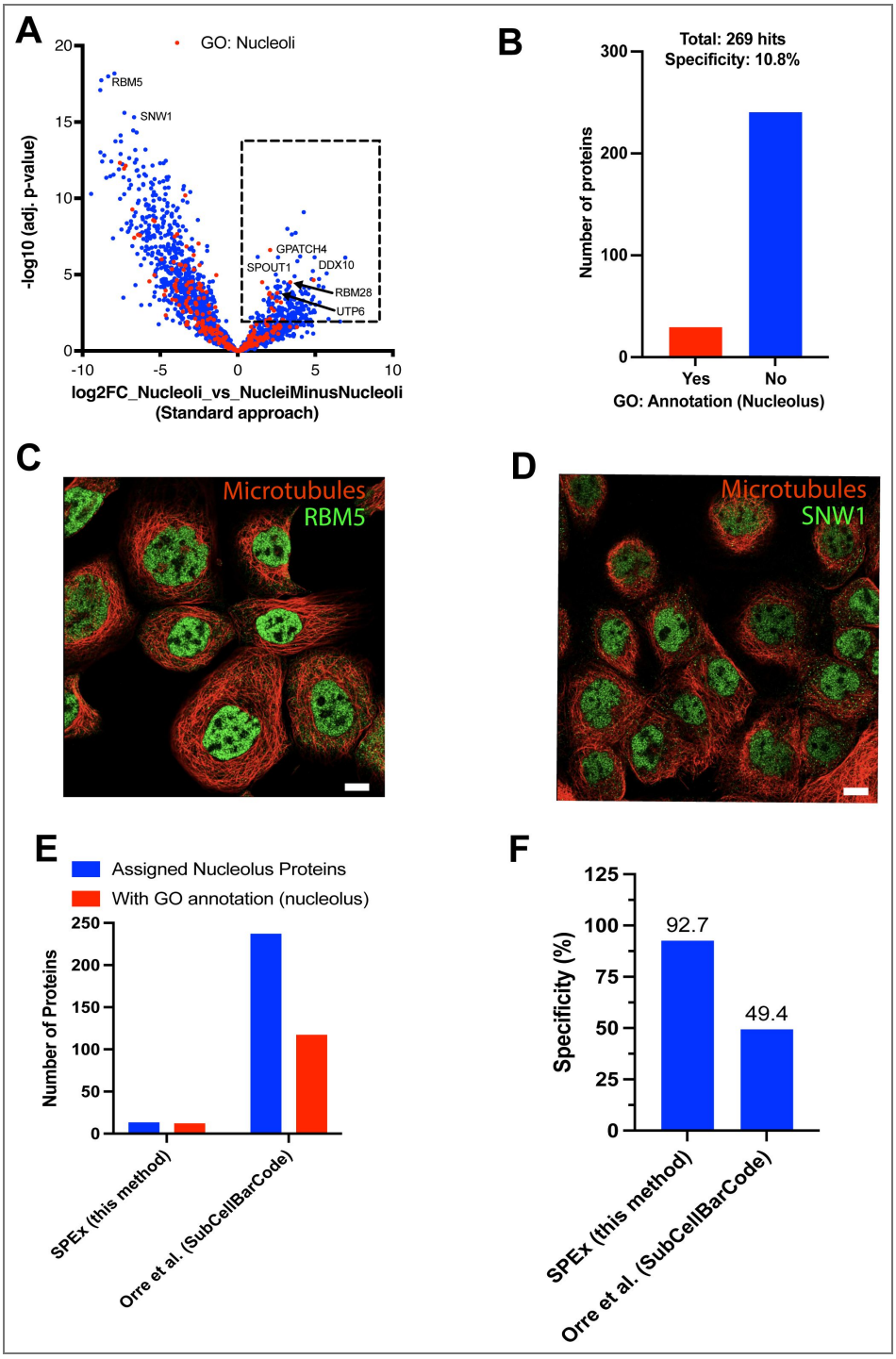

Figure S2.

(**A**) Volcano plot of pairwise proteomic comparison between nucleoli and NucleiMinusNucleoli. The dotted square indicates proteins significantly enriched in nucleoli (adjusted $P < 0.05$, $\log_2FC > 0$). Red dots represent proteins annotated to localize to the nucleolus according to GO. **(B)** Number of proteins significantly enriched in nucleoli in (A, dotted square) that are annotated as nucleolar (Yes) or not (No) according to GO. **(C)** A-431 cells immunostained for RBM5 and tubulin. Image adapted from Protein Atlas (*www.proteinatlas.org*). Scale bar, 10 µm. **(D)** A-431 cells immunostained for SNW1 and tubulin. Image adapted from Protein Atlas (*www.proteinatlas.org*). Scale bar, 10 µm. **(E)** Bar plot comparing the number of proteins assigned to the nucleolus (blue) in our SPEx dataset (this study, A) with the published proteomics dataset (Orre et al., 2019). Proteins overlapping with nucleolar GO annotation are shown in red. **(F)** Specificity of nucleolar GO annotation in the different proteomics datasets, determined from (E).

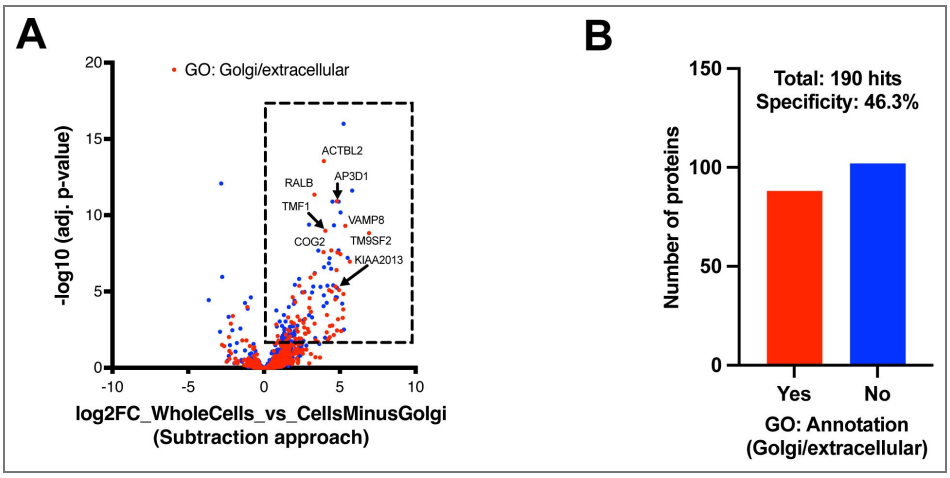

Figure S3.

(**A**) Volcano plot of pairwise proteomic comparison between WholeCells and CellsMinusGolgi. The dotted square indicates proteins significantly enriched (adjusted $P < 0.05$, $\log_2FC > 0$) in the WholeCells. Red dots represent proteins annotated to localize to the Golgi and/or to be extracellular according to GO. **(B)** Number of proteins significantly enriched in the Golgi in (A) that are annotated as Golgi and/or extracellular (Yes) or not (No) according to GO.

Data availability

All data are included in the main text or supplementary. All mass spectrometry proteomics data associated with this manuscript have been deposited to the ProteomicsXchange consortium via MassIVE (*https://massive.ucsd.edu*) with the accession number MSV000101122/PXD075606.

Acknowledgements

This work was a collaboration between the Spang Lab, the Imaging Core Facility and the Proteomics Core Facility (all Biozentrum, Basel). The authors thank Dariush Mollet for his valuable assistance with data analysis, preparation of figures, and contributions to the methods section. We also thank the Hondele lab (Biozentrum, Basel) for providing antibodies against NCL and SON and the Spiess lab (former Biozentrum, Basel) for sharing the HeLa CCL2 cell line. Finally, we thank Paul Guichard and Virginie Hamel's lab (Université de Genève) and the FAME facility (FMI, Basel), especially Sabine Reither for productive discussions on expansion protocol optimization. This work was supported by the University of Basel and the Swiss National Science Foundation (310030_197779, 310030_219513, 320030-231859) to A. Spang.

Additional information

Author Contributions

ASpa, CAF, ASch, AF and OB conceived the project. CAF, AF and ASch acquired the data. ASch, CAF, ASpa and AF analyzed and interpreted the data. CAF, ASpa, and ASch wrote the manuscript. All authors commented on the manuscript.

Funding

Funder	Grant reference number	Author
Universität Basel (UB)		Alexia Ferrand Curdin A Franziscus Oliver Biehlmaier Anne Spang Alexander Schmidt
Schweizerischer Nationalfonds zur Förderung der Wissenschaftlichen Forschung (SNF)	310030_197779	Anne Spang
Schweizerischer Nationalfonds zur Förderung der Wissenschaftlichen Forschung (SNF)	310030_219513	Anne Spang
Schweizerischer Nationalfonds zur Förderung der Wissenschaftlichen Forschung (SNF)	320030-231859	Anne Spang

Author ORCID iDs

Alexia Ferrand: https://orcid.org/0000-0001-7292-1325
Alexander Schmidt: https://orcid.org/0000-0002-3149-2381
Anne Spang: https://orcid.org/0000-0002-2387-6203

Additional files

Supplementary file 1. Supplementary tables.

Supplementary video 1. Subcellular laser microdissection of different samples Example movies of laser microdissection for all samples shown in Figure 2E. The movies are shown at 3x speed.

References

1. **Bhat P,** Chow A, Emert B, Ettlin O, Quinodoz SA, Strehle M, Takei Y, Burr A, Goronzy IN, Chen AW, *et al.* (2024) Genome organization around nuclear speckles drives mRNA splicing efficiency. *Nature* **629**:1165-1173 https://doi.org/10.1038/s41586-024-07429-6 | PubMed
2. **Brunner A,** Thielert M, Vasilopoulou C, Ammar C, Coscia F, Mund A, Hoerning OB, Bache N, Apalategui A, Lubeck M, *et al.* (2022) Ultra-high sensitivity mass spectrometry quantifies single-cell proteome changes upon perturbation. *Molecular Systems Biology* **18**:MSB202110798 https://doi.org/10.15252/msb.202110798 | PubMed
3. **Chang H-J,** Cheung CHY, Chong WM, Lu H-H. (no date) Microscoop®: Two Photon-induced Biotinylation of Protein Constituents with Submicron Specificity.
4. **Chen F,** Tillberg PW, Boyden ES (2015) Expansion microscopy. *Science* **347**:543-548 https://doi.org/10.1126/science.1260088 | PubMed
5. **Chen Y-D,** Chang C-W, Cheung CHY, Chang H-J, Sie Y-D, Chung C-W, Huang C-K, Huang C-C, Chong WM, Liu Y-P, *et al.* (2023) Microscopy-guided subcellular proteomic discovery by high-speed ultra-content photo-biotinylation. *bioRxiv* https://doi.org/10.1101/2023.12.27.573388
6. **Cho NH,** Cheveralls KC, Brunner A-D, Kim K, Michaelis AC, Raghavan P, Kobayashi H, Savy L, Li JY, Canaj H, *et al.* (2022) OpenCell: proteome-scale endogenous tagging enables the cartography of human cellular organization. *Science* **375**:eabi6983 https://doi.org/10.1126/science.abi6983 | PubMed
7. **Damstra HG,** Mohar B, Eddison M, Akhmanova A, Kapitein LC, Tillberg PW (2022) Visualizing cellular and tissue ultrastructure using Ten-fold Robust Expansion Microscopy (TREx). *eLife* **11**:e73775 https://doi.org/10.7554/eLife.73775 | PubMed
8. **Domazet B,** MacLennan GT, Lopez-Beltran A, Montironi R, Cheng L (2008) Laser Capture Microdissection in the Genomic and Proteomic Era: Targeting the Genetic Basis of Cancer. *International Journal of Clinical and Experimental Pathology* **1**:475-488 PubMed
9. **Dong Z,** Jiang W, Wu C, Chen T, Chen J, Ding X, Zheng S, Piatkevich KD, Zhu Y, Guo T (2024) Spatial proteomics of single cells and organelles on tissue slides using filter-aided expansion proteomics. *Nature Communications* **15**:9378 https://doi.org/10.1038/s41467-024-53683-7 | PubMed
10. **Fasimoye R,** Dong W, Nirujogi RS, Rawat ES, Iguchi M, Nyame K, Phung TK, Bagnoli E, Prescott AR, Alessi DR, *et al.* (2023) Golgi-IP, a tool for multimodal analysis of Golgi molecular content. *Proceedings of the National Academy of Sciences of the United States of America* **120**:e2219953120 https://doi.org/10.1073/pnas.2219953120 | PubMed
11. **Gambarotto D,** Zwettler FU, Le Guennec M, Schmidt-Cernohorska M, Fortun D, Borgers S, Heine J, Schloetel J-G, Reuss M, Unser M, *et al.* (2019) Imaging cellular ultrastructures using expansion microscopy (U-ExM). *Nature Methods* **16**:71-74 https://doi.org/10.1038/s41592-018-0238-1 | PubMed
12. **Geladaki A,** Kočevar Britovšek N, Breckels LM, Smith TS, Vennard OL, Mulvey CM, Crook OM, Gatto L, Lilley KS (2019) Combining LOPIT with differential ultracentrifugation for high-resolution spatial proteomics. *Nature Communications* **10**:331 https://doi.org/10.1038/s41467-018-08191-w | PubMed
13. **Guzman UH,** Martinez-Val A, Ye Z, Damoc E, Arrey TN, Pashkova A, Renuse S, Denisov E, Petzoldt J, Peterson AC, *et al.* (2024) Ultra-fast label-free quantification and comprehensive proteome coverage with narrow-window data-independent acquisition. *Nature Biotechnology* **42**:1855-1866 https://doi.org/10.1038/s41587-023-02099-7 | PubMed
14. **Hein MY,** Peng D, Todorova V, McCarthy F, Kim K, Liu C, Savy L, Januel C, Baltazar-Nunez R, Sekhar M, *et al.* (2025) Global organelle profiling reveals subcellular localization and remodeling at proteome scale. *Cell* **188**:1137-1155.e20. https://doi.org/10.1016/j.cell.2024.11.028 | PubMed
15. **Herrera JA,** Mallikarjun V, Rosini S, Montero MA, Lawless C, Warwood S, O'Cualain R, Knight D, Schwartz MA, Swift J (2020) Laser capture microdissection coupled mass spectrometry (LCM-MS) for spatially resolved analysis of formalin-fixed and stained human lung tissues. *Clinical Proteomics* **17**:24 https://doi.org/10.1186/s12014-020-09287-6 | PubMed

16. **Hondele M,** Sachdev R, Heinrich S, Wang J, Vallotton P, Fontoura BMA, Weis K (2019) DEAD-box ATPases are global regulators of phase-separated organelles. *Nature* **573**:144-148 https://doi.org/10.1038/s41586-019-1502-y | PubMed

17. **Hundley FV,** Gonzalez-Lozano MA, Gottschalk LM, Cook ANK, Zhang J, Paulo JA, Harper JW (2024) Endo-IP and lyso-IP toolkit for endolysosomal profiling of human-induced neurons. *Proceedings of the National Academy of Sciences* **121**:e2419079121 https://doi.org/10.1073/pnas.2419079121 | PubMed

18. **Krautbauer S,** Neumeier M, Haberl EM, Pohl R, Feder S, Eisinger K, Rein-Fischboeck L, Buechler C (2019) The utrophin–beta 2 syntrophin complex regulates adipocyte lipid droplet size independent of adipogenesis. *Molecular and Cellular Biochemistry* **452**:29-39 https://doi.org/10.1007/s11010-018-3409-6 | PubMed

19. **Large TYSL,** Mantini G, Meijer LL, Pham TV, Funel N, Grieken NCT van, Kok B, Knol J, Laarhoven HWM van, Piersma SR, *et al.* (2020) Microdissected pancreatic cancer proteomes reveal tumor heterogeneity and therapeutic targets. *JCI Insight* **5** https://doi.org/10.1172/jci.insight.138290 | PubMed

20. **Liffner B,** Silva TLA e, Vega-Rodriguez J, Absalon S. (2024) Mosquito Tissue Ultrastructure-Expansion Microscopy (MoTissU-ExM) enables ultrastructural and anatomical analysis of malaria parasites and their mosquito. *BMC Methods* **1**:13 https://doi.org/10.1186/s44330-024-00013-4 | PubMed

21. **Lundberg E,** Borner GHH (2019) Spatial proteomics: a powerful discovery tool for cell biology. *Nature Reviews Molecular Cell Biology* **20**:285-302 https://doi.org/10.1038/s41580-018-0094-y | PubMed

22. **Makhmut A,** Dragomir MP, Fritzsche S, Moebs M, Schmitt WD, Taube ET, Coscia F (2026) Spatial proteomics of ovarian cancer precursors delineates early disease changes and drug targets. *Molecular Systems Biology* **22**:7-41 https://doi.org/10.1038/s44320-025-00168-4 | PubMed

23. **Nirschl JJ,** Magiera MM, Lazarus JE, Janke C, Holzbaur ELF (2016) α-Tubulin Tyrosination and CLIP-170 Phosphorylation Regulate the Initiation of Dynein-Driven Transport in Neurons. *Cell Reports* **14**:2637-2652 https://doi.org/10.1016/j.celrep.2016.02.046 | PubMed

24. **Orre LM,** Vesterlund M, Pan Y, Arslan T, Zhu Y, Fernandez Woodbridge A, Frings O, Fredlund E, Lehtiö J (2019) SubCellBarCode: Proteome-wide Mapping of Protein Localization and Relocalization. *Molecular Cell* **73**:166-182.e7. https://doi.org/10.1016/j.molcel.2018.11.035 | PubMed

25. **Perez F,** Diamantopoulos GS, Stalder R, Kreis TE (1999) CLIP-170 Highlights Growing Microtubule Ends In Vivo. *Cell* **96**:517-527 https://doi.org/10.1016/S0092-8674(00)80656-X | PubMed

26. **Rosenberger FA,** Mädler SC, Thorhauge KH, Steigerwald S, Fromme M, Lebedev M, Weiss CAM, Oeller M, Wahle M, Metousis A, *et al.* (2025) Deep Visual Proteomics maps proteotoxicity in a genetic liver disease. *Nature* **642**:484-491 https://doi.org/10.1038/s41586-025-08885-4 | PubMed

27. **Rosenberger FA,** Thielert M, Strauss MT, Schweizer L, Ammar C, Mädler SC, Metousis A, Skowronek P, Wahle M, Madden K, *et al.* (2023) Spatial single-cell mass spectrometry defines zonation of the hepatocyte proteome. *Nature Methods* **20**:1530-1536 https://doi.org/10.1038/s41592-023-02007-6 | PubMed

28. **Roux KJ,** Kim DI, Raida M, Burke B (2012) A promiscuous biotin ligase fusion protein identifies proximal and interacting proteins in mammalian cells. *Journal of Cell Biology* **196**:801-810 https://doi.org/10.1083/jcb.201112098 | PubMed

29. **Schessner JP,** Albrecht V, Davies AK, Sinitcyn P, Borner GHH (2023) Deep and fast label-free Dynamic Organellar Mapping. *Nature Communications* **14**:5252 https://doi.org/10.1038/s41467-023-41000-7 | PubMed

30. **Sheard TMD,** Shakespeare TB, Seehra RS, Spencer ME, Suen KM, Jayasinghe I (2023) Differential labelling of human sub-cellular compartments with fluorescent dye esters and expansion microscopy. *Nanoscale* **15**:18489-18499 https://doi.org/10.1039/D3NR01129A | PubMed

31. **Su H,** Kodiha M, Lee S, Stochaj U (2013) Identification of Novel Markers That Demarcate the Nucleolus during Severe Stress and Chemotherapeutic Treatment. *PLoS ONE* **8**:e80237 https://doi.org/10.1371/journal.pone.0080237 | PubMed

32. **Szklarczyk D,** Nastou K, Koutrouli M, Kirsch R, Mehryary F, Hachilif R, Hu D, Peluso ME, Huang Q, Fang T, *et al.* (2025) The STRING database in 2025: protein networks with directionality of regulation. *Nucleic Acids Research* **53**:D730-D737 https://doi.org/10.1093/nar/gkae1113 | PubMed

33. (no date) The Human Protein Atlas. https://www.proteinatlas.org/

34. **The UniProt Consortium** (2025) UniProt: the Universal Protein Knowledgebase in 2025. *Nucleic Acids Research* **53**:D609-D617 https://doi.org/10.1093/nar/gkae1010 | PubMed

35. **Thul PJ,** Åkesson L, Wiking M, Mahdessian D, Geladaki A, Ait Blal H, Alm T, Asplund A, Björk L, Breckels LM, *et al.* (2017) A subcellular map of the human proteome. *Science* **356**:eaal3321 https://doi.org/10.1126/science.aal3321 | PubMed

36. **Tillberg PW,** Chen F, Piatkevich KD, Zhao Y, Yu C-C (Jay), English BP, Gao L, Martorell A, Suk H-J, Yoshida F, *et al.* (2016) Protein-retention expansion microscopy of cells and tissues labeled using standard fluorescent proteins and antibodies. *Nature Biotechnology* **34**:987-992 https://doi.org/10.1038/nbt.3625 | PubMed

37. **Walavalkar K,** Gupta S, Kresoja-Rakic J, Raingeval M, Mungo C, Rubin P, Santoro R (2025) Single-cell dynamics of genome-nucleolus interactions captured by nucleolar laser microdissection (NoLMseq). *Nature Communications* **16**:11417 https://doi.org/10.1038/s41467-025-66294-7 | PubMed

38. **Wen G,** Leen V, Rohand T, Sauer M, Hofkens J (2023) Current Progress in Expansion Microscopy: Chemical Strategies and Applications. *Chemical Reviews* **123**:3299-3323 https://doi.org/10.1021/acs.chemrev.2c00711 | PubMed

Peer reviews

Reviewer #1 (Public review):

Summary:

The authors present a novel approach to subcellular spatial proteomics by combining laser microdissection with expansion microscopy and LC-MS/MS analysis (SPEx). They implement two different workflows for LMD and LC-MS/MS quantification:

(1)The standard approach, where an area of interest is cut out by LMD, subjected to proteomics analysis, and compared to the rest of the cell without the dissected ROI.

(2) The subtraction approach, where ROIs are removed, and the remaining cellular material is compared to samples containing both the surrounding material and the ROI.

The authors assess the technique by applying it to subcellular targets of various sizes, volumes, and protein compositions such as the nucleus, nucleoli, and Golgi. They demonstrate that SPEx can identify proteins enriched or reduced in ROIs.

Strengths:

The broad, relatively easy, and inexpensive applicability of this approach to potentially many cell types and subcellular areas of interest provides an exciting alternative to subcellular fractionation, native immunoprecipitation, or genetically encoded proximity labeling constructs. Moreover, by visually selecting ROIs for subsequent analysis, subcellular context or organelle morphology can be taken into account, as discussed by the authors in the discussion section.

Weaknesses:

While strongly supporting the sharing of this approach, we have a number of comments and questions that will improve the impact of the manuscript:

(1) General:

a) The manuscript would benefit from restructuring and language revision. In its current form, the writing is sometimes dense and verbose (in particular, the Results section). This makes it difficult to follow the authors' arguments.

b) The authors mention the possibility of selecting organelles based on morphology. This is left for the discussion, but it seems like a missed opportunity - the authors could compare individual organelles in different morphological states, e.g., connected vs. fragmented mitochondria.

(2) Technical:

a) Why do the authors strive and optimize for a 10x expansion factor? Is SPEx compatible with a more standard 4x expansion, as e.g., used in the classic U-ExM approach (*https://www.nature.com/articles/s41592-018-0238-1)?* This could be added to the discussion.

b) The U-ExM approach shows improved ultrastructural preservation when using 3%FA with 0.1% glutaraldehyde fixation (GA). Is SPEx compatible with the use of low amounts of GA for fixation?

c) Related to the above, was the anchoring efficiency reduced only to achieve a 10x expansion factor or does this additionally affect the proteome coverage?

d) Have the authors considered using alternative anchoring approaches, such as GMA (*https://journals.plos.org/plosone/article?id=10.1371/journal.pone.0291506#pone.0291506.s001*), which potentially increase the amount of sample retained in the hydrogel, thus allowing for better proteome coverage? This could be added to the discussion.

e) The limitation of the approach to near-2D samples should be mentioned, and alternative approaches for more 3D samples could be discussed.

f) How are peptides that are directly anchored to the hydrogel dealt with during LC-MS/MS analysis? Are they excluded, or can they be identified during the spectral search? The latter would allow us to get a deeper structural understanding of how proteins are actually anchored into hydrogels, which so far has not been assessed.

An alternative approach to address this question would be to investigate if the peptide coverage of proteins detected by SPEx is enriched for peptides representing the folded core of proteins as opposed to the surface-exposed regions, which likely get more anchored into the hydrogel.

g) Same question regarding peptides with NHS labeling. Can they be identified, or do they just compete for ionization and thus negatively affect coverage and dynamic range of the LC-MS/MS approach?

h) How are the primary and secondary antibodies affecting the proteomics analysis identified as contaminants?

i) Have the authors observed differences in proteomics coverage of only antibody vs NHS-labeling? Depending on the questions above, could pure antibody-based labeling increase proteomic coverage?

https://doi.org/10.7554/eLife.111393.1.sa2

Reviewer #2 (Public review):

Summary:

This study introduces a method that combines physical expansion of cells, imaging-guided isolation of defined regions, and protein identification to enable compartment-resolved analysis of protein composition at the subcellular scale. The authors aim to address a central limitation in existing approaches, namely the loss of spatial information during sample preparation or the indirect nature of proximity-based labeling methods. Using several cellular compartments as examples, they demonstrate that their approach can recover compartment-enriched protein sets and identify candidate proteins with previously unassigned localization.

Strengths:

A major strength of this work is the conceptual simplicity and accessibility of the approach. By combining established techniques in a modular way, the method avoids the need for genetic manipulation or specialized labeling strategies, making it broadly adaptable across experimental systems. The ability to directly select regions of interest based on imaging represents a clear advantage over indirect enrichment strategies and allows flexible targeting of both membrane-bound and non-membrane-bound compartments.

The experimental design is also a strong aspect of the study. The use of complementary comparison strategies-analyzing isolated compartments alongside matched "subtracted" controls-provides an internal framework for assessing enrichment and depletion, increasing confidence in spatial assignment. The application of the method across multiple organelles of different sizes and properties demonstrates versatility, and the reported specificity for several compartments is encouraging. In particular, the ability to profile small and biochemically challenging structures highlights a potentially important niche for the approach.

Weaknesses:

Despite these strengths, several methodological limitations constrain the interpretation of the results. The most important relates to spatial accuracy in three dimensions. While lateral resolution is improved through physical expansion, the lack of depth resolution introduces uncertainty regarding contributions from structures above and below the selected region. Although the authors argue that this does not substantially affect specificity, the current evidence is largely indirect, and a more rigorous quantification of potential contamination would strengthen this conclusion.

Quantitative interpretation also remains challenging. Because the measurements reflect total protein abundance rather than local concentration, differences in compartment size and protein density can influence enrichment values, particularly for small structures embedded within larger volumes. This issue is evident in the analysis of smaller compartments and complicates direct comparison across conditions. Additional normalization or modeling would help clarify how to interpret these measurements.

Another limitation concerns variability in the expansion process and its downstream consequences. Differences in expansion factor across samples may affect the definition of regions of interest and introduce variability in sampling, yet the impact of this variability is not fully explored. Similarly, the use of a modified chemical treatment to preserve proteins for downstream analysis is central to the workflow but is not extensively validated with respect to preservation of spatial organization.

While the identification of previously unannotated proteins is an appealing aspect of the study, validation is limited to a small number of examples, and broader support from independent datasets or literature context is lacking. In addition, the study primarily focuses on steady-state measurements in a single cell type, and therefore does not yet demonstrate

the ability of the method to capture dynamic or condition-dependent changes in protein localization.

Finally, the positioning of the method relative to existing approaches could be more clearly articulated. Although qualitative comparisons are provided, a more systematic and quantitative benchmarking against alternative strategies would help readers better understand the specific advantages and trade-offs.

https://doi.org/10.7554/eLife.111393.1.sa1

Reviewer #3 (Public review):

Franziscus et al. describe an elegant approach for spatially specific proteome analysis. To achieve this, they expand fixed cells and subsequently use a laser to micro-dissect a region of interest, which is then analyzed by mass spectrometry.

They demonstrate the effectiveness of their approach by analyzing the nucleus, nucleolus, and the Golgi, and benchmark their hits against previous datasets for these organelles.

The manuscript is very well written and nicely guides the reader through the applied methods. The presented data is convincing, and I do not see the need for additional experimental verification of the protocol. The only minor concern is the novelty of the method and the presentation. A combination of expansion, laser microdissection, and proteomics has been applied in the past (PMID: 36450705, PMID: 39477916). In the manuscript, one of these studies is cited, though it does not become clear that this approach is already described. However, Franziscus et al. describe the approach better and make it more accessible to the reader, especially since the other studies described this methodology in combination with tissue expansion and not in combination with single cell expansion as it is done here. I would ask the authors to be clearer in the introduction about what others have already done and what their contribution is here. In general, I am convinced that the community will benefit from the presented protocol to analyze organelle proteomics in detail.

https://doi.org/10.7554/eLife.111393.1.sa0

Author Response:

> ***Reviewer #1 (Public review):***
>
> *Summary:*
>
> *The authors present a novel approach to subcellular spatial proteomics by combining laser microdissection with expansion microscopy and LC-MS/MS analysis (SPEx). They implement two different workflows for LMD and LC-MS/MS quantification:*
>
> *(1)The standard approach, where an area of interest is cut out by LMD, subjected to proteomics analysis, and compared to the rest of the cell without the dissected ROI.*
>
> *(2) The subtraction approach, where ROIs are removed, and the remaining cellular material is compared to samples containing both the surrounding material and the ROI.*
>
> *The authors assess the technique by applying it to subcellular targets of various sizes, volumes, and protein compositions such as the nucleus, nucleoli, and Golgi. They demonstrate that SPEx can identify proteins enriched or reduced in ROIs.*
>
> *Strengths:*

> *The broad, relatively easy, and inexpensive applicability of this approach to potentially many cell types and subcellular areas of interest provides an exciting alternative to subcellular fractionation, native immunoprecipitation, or genetically encoded proximity labeling constructs. Moreover, by visually selecting ROIs for subsequent analysis, subcellular context or organelle morphology can be taken into account, as discussed by the authors in the discussion section.*
>
> *Weaknesses:*
>
> *While strongly supporting the sharing of this approach, we have a number of comments and questions that will improve the impact of the manuscript:*

We thank the reviewer for the careful evaluation of our manuscript and the generally positive assessment. We plan on improving our manuscript based on the reviewers' comments.

> *(1) General:*
>
> *a) The manuscript would benefit from restructuring and language revision. In its current form, the writing is sometimes dense and verbose (in particular, the Results section). This makes it difficult to follow the authors' arguments.*

We will improve readability and clarity of the results section in the revised manuscript.

> *b) The authors mention the possibility of selecting organelles based on morphology. This is left for the discussion, but it seems like a missed opportunity - the authors could compare individual organelles in different morphological states, e.g., connected vs. fragmented mitochondria.*

The authors agree with the reviewers' assessment that investigating proteome of organelles based on morphology or cellular state is an exciting application of SPEx. While we plan experiments along this line in the future, we think that these experiments are beyond the scope of this manuscript, which is meant to describe the method and its general usefulness.

> *(2) Technical:*
>
> *a) Why do the authors strive and optimize for a 10x expansion factor? Is SPEx compatible with a more standard 4x expansion, as e.g., used in the classic U-ExM approach (https://www.nature.com/articles/s41592-018-0238-1)? This could be added to the discussion.*

We aimed for 10x expansion solely because our ultimate goal is to cut out very small structures. Isolating structures as small as nucleoli would not be as reliable with a lower expansion factor (i.e. 4x) expansion. We did not assess the compatibility with U-ExM. We would assume that SPEx would also work with U-ExM as expansion method; omitting protease treatment, however. Still, we performed pilots with just 4x expansion (using TREx) in the early stages of optimization. We were able to isolate single cells and obtain similar protein coverage as with 10x expansion. We will further clarify our motivation to use 10x expansion in the discussion.

We would also like to point out whether to U-ExM the standard method or not is rather subjective. Even though TREx was published three years later, it is also very widely used. The original expansion microscopy method was published three years prior to U-ExM.

> *b) The U-ExM approach shows improved ultrastructural preservation when using 3%FA with 0.1% glutaraldehyde fixation (GA). Is SPEx compatible with the use of low amounts of GA for fixation?*

We tried different fixation methods in the early stages of this study (where expansion was not yet close to 10x). We saw a mild negative effect of GA on the expansion factor, so we avoided it in the later experiments since it also did not seem necessary to preserve the structure of our organelles of interest. However, the use of GA would generally be compatible with SPEx, potentially at the cost of a mild negative effect on expansion factor (see Author response image 1) and proteome coverage. We can add this information to the discussion.

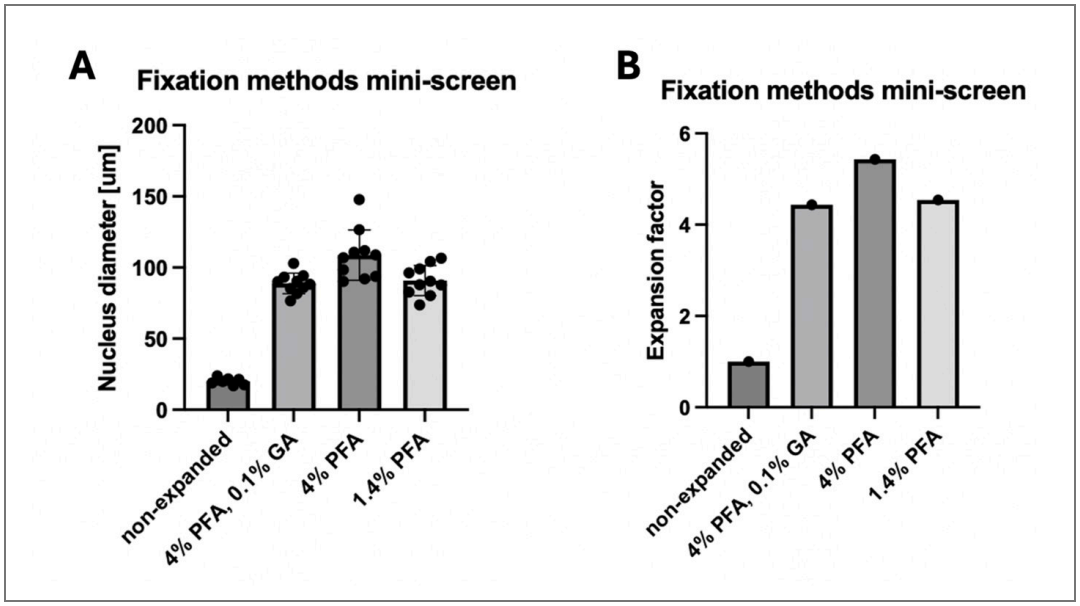

Author response image 1. Fixation methods mini-screen. Cells were fixed with the indicated reagents for 10 minutes at 37°C. After TREx expansion, the diameter of the nucleus was measured (A) and the resulting expansion factor compared to the non-expanded control was determined (B).

> *Related to the above, was the anchoring efficiency reduced only to achieve a 10x expansion factor or does this additionally affect the proteome coverage?*

We solely lowered the anchoring in order to allow for higher expansion factors. In earlier pilots we performed proteomic analysis on samples that were just expanded 4x using standard TREx expansion (also using the original anchoring strategy from the TREx publication, consisting of 0.2 mg/ml AcX for overnight at RT). We presented the results of this pilot in Fig S1A. We still detected over 2,000 proteins from 10 cells, a coverage, which is highly similar to what we found in the final experiments (Figure 2F), in which the anchoring was lower yielding 10x expansion. Based on these data, we hypothesize that anchoring (and expansion factor!) has a negligible impact on protein coverage. We will clarify this in the manuscript.

> *d) Have the authors considered using alternative anchoring approaches, such as GMA (https://journals.plos.org/plosone/article?id=10.1371/journal.pone.0291506#pone.0291506.s001), which potentially increase the amount of sample retained in the hydrogel, thus allowing for better proteome coverage? This could be added to the discussion.*

We did not use alternative anchoring approaches. We modified the TREx protocol to fit our purposes and since this was sufficient, we did not explore alternatives. However, using anchoring approaches, in which higher amounts of sample could be retained in the gel might be beneficial for the proteomics coverage. We will keep this suggestion in mind for future experiments. Thank you for the suggestion!

> *e) The limitation of the approach to near-2D samples should be mentioned, and alternative approaches for more 3D samples could be discussed.*

The authors agree that SPEx is limited to near-2D samples at this point. We suggest that SPEx is applicable for 3D samples (e.g. in tissues) by performing cryosectioning. TREx has been shown to be compatible with sectioned tissue (Damstra et al., 2022). We will elaborate this in the discussion.

> *f) How are peptides that are directly anchored to the hydrogel dealt with during LC-MS/MS analysis? Are they excluded, or can they be identified during the spectral search? The latter would allow us to get a deeper structural understanding of how proteins are actually anchored into hydrogels, which so far has not been assessed.*

The reviewer raises an interesting point. In general, peptides carrying the anchoring modification are analysed by LC-MS, but we did not include these specific modifications in the database search. Overall, we assumed that the labeling would be low and stochastic and hence should, if at all, only minimally affect the detection of peptides. Nevertheless, in response to the reviewers' comment, we searched the MS data again for the crosslinking reagent linked to lysine residues. However, we could not get any confident hit for any peptide containing this modification. Since we cannot exclude that the modification precludes the identification of the corresponding peptides, we compared the number peptides generated by trypsin cleavage after arginine and lysine. As the human genome contains similar proportions of both amino acids, one would expect similar numbers of both peptide types being identified. Any modifications of lysine by the anchoring reagent used, would prevent tryptic cleavage and thus reduce the number of lysine peptides. As shown in Author response image 2, the number of lysine terminating is only slightly lower compared to arginine terminating peptides. Notably, the proteomics results of a different fixed human tissue sample directly extracted by laser capture micro dissection without expansion showed a very similar lysine to arginine peptide ratio. This indicates that the large majority of lysine residues is not modified and affected by the hydrogel anchoring.

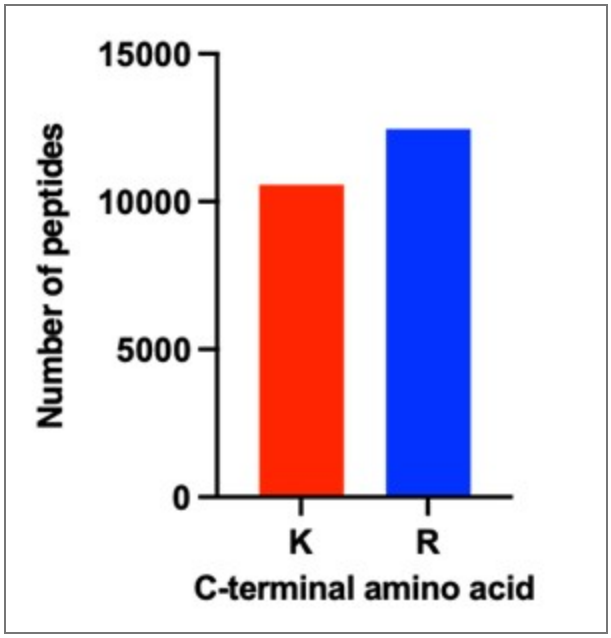

Author response image 2. Number of peptides identified either terminating with lysine (K) or arginine (R) across all samples shown in Figure 5F.

> *An alternative approach to address this question would be to investigate if the peptide coverage of proteins detected by SPEx is enriched for peptides representing the folded core of proteins as opposed to the surface-exposed regions, which likely get more anchored into the hydrogel.*

Because of the negligible amounts of modified peptides, we did not investigate this potential bias of surface-exposed versus folded-core peptides.

> *g) Same question regarding peptides with NHS labeling. Can they be identified, or do they just compete for ionization and thus negatively affect coverage and dynamic range of the LC-MS/MS approach?*

The reviewer raises a similar point as above for another lysine labeling used during the SPEx protocol. Again, we specifically looked for this modification by re-searching the raw MS data, but still could not identify any peptides, carrying this modification on a lysine residue. Even though we cannot exclude that this rather large modification prevents detection, considering the high number of lysine terminating peptides in our dataset (see Figure 2), we would expect that also this labeling step is stochastic and affects only a minor proportion of the proteins.

> *h) How are the primary and secondary antibodies affecting the proteomics analysis identified as contaminants?*

We thank the reviewer for this comment. Since antibodies bind to proteins in a non-covalent manner, they will be released during the denaturing steps of the protocol. Of course, the antibodies will stay in the sample, be digested and analyzed and could, if very abundant, affect the analysis of the proteins from the samples. To check this possibility, we re-searched the MS data including the sequences of the antibodies used. To our surprise, we could not detect any peptides of these antibodies. This suggests that the concentrations of the antibodies used are much lower than those of the sample proteins and thus should not have any impact on the proteomics results. We interpret this result also as a benefit of our method compared to organellar-IP.

> *i) Have the authors observed differences in proteomics coverage of only antibody vs NHS-labeling? Depending on the questions above, could pure antibody-based labeling increase proteomic coverage?*

We did not perform this comparative analysis, since we always used NHS dyes. In the experiments presented in this manuscript, NHS dyes allowed easy visualization of the whole cell without the use of antibodies. This NHS staining was essential for this particular setup for sample acquisition. We cut out entire cells, cells lacking the nucleus and cells lacking the Golgi apparatus, which served as critical controls. However, other ways of detecting cell boundaries could be used to avoid NHS staining. As shown above, both, the anchor and NHS labeling are likewise sparse and stochastic. Moreover, we could not detect any impact of the antibody labeling to our results. Thus, we assume that both labeling procedures could be used.

> ***Reviewer #2 (Public review):***
>
> *Summary:*
>
> *This study introduces a method that combines physical expansion of cells, imaging-guided isolation of defined regions, and protein identification to enable compartment-resolved analysis of protein composition at the subcellular scale. The authors aim to address a central limitation in existing approaches, namely the loss of spatial information during sample preparation or the indirect nature of proximity-based labeling methods. Using several cellular compartments as examples, they demonstrate*

https://doi.org/10.7554/eLife.111393.1.sa4